Environmental Chemistry Letters (2019) 17:655–682
https://doi.org/10.1007/s10311-018-0814-8

REVIEW

Carbon nitride, metal nitrides, phosphides, chalcogenides, perovskites and carbides nanophotocatalysts for environmental applications

Amit Kumar[1,2,3] · Priya Rittika Thakur[3] · Gaurav Sharma[1,2] · Mu. Naushad[4] · Anamika Rana[3] · Genene Tessema Mola[5] · Florian J. Stadler[1]

Received: 16 April 2018 / Accepted: 5 September 2018 / Published online: 3 October 2018

Abstract
Effective technologies and materials are needed for environmental detoxification and clean energy production. The actual photocatalytic technology is largely dependent on metal oxide-based semiconductors, which have issues such as cost, limited spectral response and recombination problems. Alternatively, non-metal photocatalysts have recently emerged. This article reviews non-metal oxide photocatalytic materials such as carbon nitride, metal nitrides, phosphides, chalcogenides, perovskites and carbides for environmental clean-up and energy production.

Keywords Environmental detoxification · Metal oxide · Alternative photocatalyst · Contaminant removal · Clean energy

Introduction

In recent years, research on highly efficient photocatalysts with multi-pronged approach has been rapidly expanding. The increasing level of human activities has led to search for alternative technologies for environmental detoxification and energy production. Especially in the field of water treatment and purification, the organic, inorganic and microbial contaminants are increasing in terms of quantity, variability and risk factors (Kumar et al. 2018a). A new range of persistent and emerging pollutants have been evolved including polycyclic hydrocarbons, endocrine disruptors and surfactants. These are primarily found in aquatic environments and contaminated water or marine sediments (Sanz et al. 2003). Considering emerging and recalcitrant pollutants as serious issue for environment and human health, many mitigation techniques are investigated. Advanced oxidation processes, especially semiconductor photocatalysis, have been utilized to a great extent. This process provides an excellent and greener path for solving the energy and pollution issues (Fujishima and Honda 1972; Serpone and Khairutdinov 1997). Till date, semiconductor materials involved for photocatalytic applications include metal oxide- and carbon-based materials (Kandavelu et al. 2004; Weng et al. 2014). In previous times, the TiO_2 photocatalysts or metal oxide photocatalysts were essentially used for the pollutant removal, hydrogen production, water splitting, inorganic synthesis and many more (Carp et al. 2004; Fujishima et al. 2000).

Although heterogeneous photocatalysis using metal oxides has been proved to be highly efficient in environmental detoxification and clean energy production, still many limitations are there. And as a result, this technology was not applicable to some processes like decontamination of highly polluted industrial liquid waste. TiO_2 has been a revolutionary photocatalyst so far, but the main disadvantage is

✉ Amit Kumar
mittuchem83@gmail.com

✉ Florian J. Stadler
fjstadler@szu.edu.cn

1 College of Materials Science and Engineering, Shenzhen Key Laboratory of Polymer Science and Technology, Guangdong Research Center for Interfacial Engineering of Functional Materials, Nanshan District Key Laboratory for Biopolymers and Safety Evaluation, Shenzhen University, Shenzhen 518060, People's Republic of China

2 Key Laboratory of Optoelectronic Devices and Systems of Ministry of Education and Guangdong Province, College of Optoelectronic Engineering, Shenzhen University, Shenzhen 518060, People's Republic of China

3 School of Chemistry, Shoolini University, Solan, Himachal Pradesh 173229, India

4 Department of Chemistry, College of Science, Building#5, King Saud University, Riyadh 11451, Saudi Arabia

5 School of Chemistry and Physics, University of KwaZulu-Natal, Pietermaritzburg Campus, Private Bag X01, Scottsville 3209, South Africa

the limited use of solar spectrum and a high recombination of charge carriers. It is due to a narrower band gap as compared to ZnO (Carp et al. 2004; Fujishima and Honda 1972; Romero et al. 1999). Due to these limitations, there is still need for the modification of metal oxide-based photocatalysts. Hence, effective photoactive results can be achieved in the visible spectrum (Carp et al. 2004; Kitano et al. 2007). From the last few years, novel photocatalysts have been synthesized and tested which are possible alternative for metal oxides. These alternative photocatalysts do not originate from the modification of metal oxides like coupling, doping or other changes, but these are totally different compounds having different structures and compositions. Novel photoactive semiconductor mixed oxides of transition metals such as V, Ta or Nb and elements like Ga, Bi or In have been investigated as alternative photocatalysts (Kudo and Miseki 2009; Maeda and Domen 2007; Osterloh 2007). Some cation interchanged zeolites with large surface area solids have also been founded, even though these do not have semiconductor properties (Anpo et al. 2009). Bimetallic and trimetallic nanoparticles, ion exchangers, doped metal oxides, zero-valent metals and hydrogel-based photocatalysts, aerogels, metal oxide- and carbon-based composites have been explored (Kant et al. 2014; Naushad et al. 2018; Sharma et al. 2016a; Singh et al. 2014).

Metal oxides have proved to be of considerable technological and environmental importance as they find role in electronics, spintronic, energy production, energy storage, biological applications and environmental detoxification (Kumar et al. 2018b, c). Figure 1 shows graphically the strategic importance of the metal oxides. Metal oxides behave as excellent photocatalysts because of their electronic structure, light absorption properties and charge transport. Here we discuss metal oxide as a photocatalyst. The higher surface area, suitable morphology, band gap stability and reusability

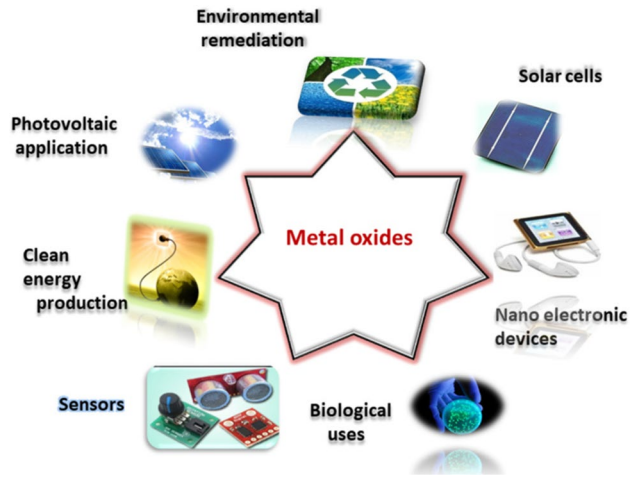

Fig. 1 Applications of metal oxides in various fields

are the features of a good photocatalytic system. However, most metal oxides as titanium oxide are active in UV region only (Wang et al. 2016). Zinc oxide (ZnO) has been used as an alternative photocatalyst to TiO_2. It has a comparable band gap, but it has a higher absorption efficiency, capturing a larger solar spectrum (Kumar et al. 2014). ZnO has been utilized in number of applications, as electronic, solar and photocatalytic processes due to its high stability, non-toxicity and electron mobility. Ong et al. reported that metal doping of ZnO improves its photocatalytic activity by reducing recombination by increasing trapping sites for electron–hole pairs (Ong et al. 2018). Many researchers have tried to improve the efficiency of these metal dioxides via doping (Dhiman et al. 2013, 2017) and forming composites with other metal oxides, etc. In addition to ZnO and TiO_2, various other metal oxides as WO_3, Al_2O_3, CwO_2, SnO_2, Co_3O_4, Bi_2O_3, etc. have been used successfully as photocatalysts. However, using these has certain disadvantages such as high cost and low quantum efficiency. The metal oxide photocatalyst not only responds to UV light but defected metal oxides also respond to visible light, and this process is widely used for environmental remediation (Ansari et al. 2013; Khan et al. 2014). This is also great milestone in the area of photocatalysis. Metal oxides are the most important class as it covers number of processes and of catalyst families which are used in industries. They are also involved in many reactions like petrochemicals, fine and pharmaceutical chemicals and biomass transformation reactions.

Limitations of metal oxides as photocatalysts

Metal oxide-based photocatalyst plays a great role in the removal of organic pollutants, saving environment, water disinfection, etc. because of its sustainable treatment technology, low cost and environmental friendly. Although advanced oxidation processes using semiconductor metal oxides have been found effective in degradation of persistent and some emerging pollutants, there is still room for further improvement and novelty. Figure 2 shows the shortcomings of a photocatalyst, which limits their use for practical and niche applications. Metal oxides possess many of these limitations. In addition, because of the valence band positions the photocatalysts suffer from the following:

- Photocorrosion and self-oxidation.
- These photocatalysts are costly, expensive and difficult to recover.
- The photocatalytic region ($\lambda < 400$ nm) of some photocatalysts is narrow such as for ZnO and TiO_2 (Kumar et al. 2014).
- There is thermal instability in the visible photocatalytic activity of particles of some photocatalysts.

- As compared to unrestricted catalysts, the photocatalytic activity of few catalysts is lower.
- Not effective on diverse kinds of pollutants.

Thus, a need of various novel photocatalysts alternative to metal oxides was felt and new photocatalysts were explored. This review focuses on different classes of photocatalysts which have been used as alternative to metal oxides or have been used for improvement of metal oxides. This is so because the use of photocatalytic technology is now just not limited to degradation of organic pollutants but is used for removal of inorganic pollutants, metal reduction, photocatalytic sensors, clean energy production, removal of NO_x, photoreduction of CO_2, photofixation of nitrates, etc. Thus, new catalysts with multi-pronged capabilities have been explored.

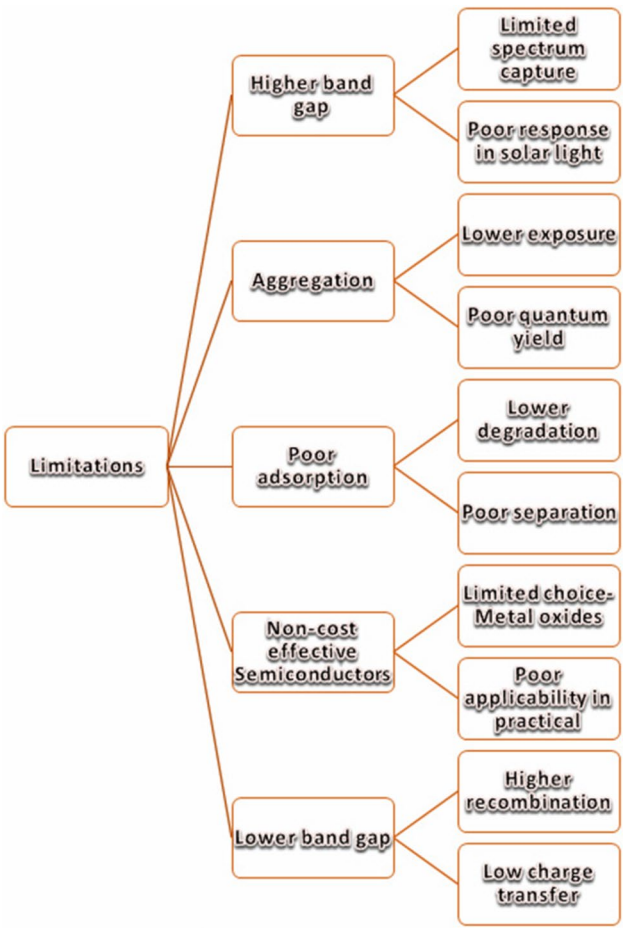

Fig. 2 Limitations of conventional photocatalysts, especially metal oxides. Each limitation has a pronounced effect on quantum efficiency and thus on the degradation rate

Alternative photocatalysts

Metal sulphides as photocatalysts

Metal sulphides being an important semiconductor class have been used in many new areas such as laser communication, light evacuated diodes and nonlinear optical devices (Yang et al. 2011). Different semiconducting metal sulphide nanomaterials have been reported to be useful for various optoelectronic devices because of their promising optical and electric properties. The metal sulphides have an empty valence band and have a quantum size effect due to their small effective mass. The above properties have a great contribution to the high charge mobility and visible light harvesting potential of metal sulphides. Many surveys have been done on the study of photoenergy conversion of metal sulphide quantum dots (QDs) including CdS, $CuInS_2$ and PbS QDs (Shen et al. 2004; Vogel et al. 1994). Depending on their particle size, the valence band and conduction band potentials of the materials are tuneable (Kondo et al. 2015; Srinivasan et al. 2015). Metal sulphides are soothed of toxic elements. Therefore, the use of metal sulphides in practical application needs the designing of metal sulphides semiconductors using safe and abundant elements. This approach is done in the way as the 'ubiquitous element strategy'. This strategy is used for the materials, used in industrial areas and bearable society (Takahashi et al. 2008). From all the elements in periodic table, we mainly focus on group IV-VI chalcogenides because they have good optoelectronic properties and high charge mobility (Ogo et al. 2008). Among these, the tin sulphides have unique characteristics, different valence numbers and sensitivity to visible light. These are used in electronic semiconductor devices and in small film solar cells (Burton et al. 2013). There are two chemical compositions of tin sulphide: (1) tin monosulphides and (2) tin disulphide.

SnS has narrow band gap than SnS_2. The electron affinity and ionization potential of SnS_2 are higher. The hydrogen production potential is smaller than the potential of SnS conduction band. The band dispersion and density of state of SnS and SnS_2 showed that these both materials are implied transition semiconductors (Zainal et al. 1996). Metal sulphide semiconductors are used for the photocatalytic hydrogen production, because these sulphides has great solar spectrum response and higher photocatalytic potential (Zhang and Guo 2013).

Cadmium sulphide nanoparticles show strong absorption in visible spectrum because of ideal band gap of 2.4 eV (Shamraiz et al. 2016). However, its low separation efficiency of charge carriers limits its use as a photocatalyst. Various attempts were made by surface modifications

as formation of nanowires, nanorods, etc. but only hollow spheres performed well in photocatalytic reactions. Fang and co-workers synthesized CdS nanoparticles with different morphologies as flowers, multi-pods, spheres and dendrites by a hydrothermal route. The photodegradation of rhodamine B was studied, and it was observed that dendrite morphology CdS exhibits highest activity. This was attributed to branched structure, small size and high surface area (Fang et al. 2017).

One of the important metal sulphides is monoclinic silver sulphide (α-Ag_2S) with a band gap of ~ 1.0 eV, which has been recently employed as photocatalysts. Silver sulphide nanoparticles are usually unstable as because of decrease in size the surface energy decreases leading to cluster formation. So it is always advisable to control the size of these nanomaterials. This has been generally used for photokilling of microbes. Recently, Ag_2S/Bi_2S_3 nanocomposites were used for photocatalytic inactivation of *E. coli* under solar light. It was found that hydroxyl radials were responsible for bacterial inactivation (Sun et al. 2013). Hu and co-workers in 2013 used solution proton alloying process for preparing mixed sulphide $NaInS_2$ with tuneable band gap and utilized for hydrogen production (Hu et al. 2016). Zinc sulphide has a wider band gap of 3.6 eV and has a lower reduction potential of about − 1.8 to − 2.0 eV (Baran et al. 2015). Many methods have been used for synthesis of ZnS as solvothermal route, reduction, thermal evaporation, hydrothermal technique, ultrasonic and microwave method (Goharshadi et al. 2013). ZnS has been used for water splitting, CO_2 reduction and organic catalytic reactions. Because of its reducing properties, it has been found suitable for photocatalytic CO_2 reduction. However, hydrogen production efficiency hinders the use of ZnS in CO_2 reduction. As a substitute to noble metals which are highly expensive, cobalt sulphide (Co_xS_y) has been used as a photocatalyst. It was reported that cobalt sulphide quantum dots enhance the electron–hole pair separation and provide active sites for hydrogen generation of 41.9 μmol h^{-1} (Yu et al. 2014). In a similar work, CdS-/Co_3S_4-coupled photocatalyst was prepared and a high H_2 production rate of 1083.9 μmol h^{-1} was achieved which was higher than noble metal-based catalyst (Zhang et al. 2018a). Copper sulphide is a well-known *p*-type semiconductor (band gap of 1.2 eV) having applications in photodegradation of pollutants, sensing, medicine and solar cells. MoS_2/Cu_2S nanomaterials were synthesized in a controlled manner with a high specific area 60.512 m^2 g^{-1}. The composite catalysts showed high activity and reusability for photodegradation of pollutants and hydrogen production (Zhang et al. 2018d).

CoS is generally not stable because of aggregation. So many reports are there where hybrid materials are used for their use as photocatalysts. Copper sulphide has a strong visible absorption and has been used for photodegradation of coloured stuff as dyes. Many metal sulphides have been successfully synthesized and utilized for various photocatalytic applications for environmental detoxification. However, the sulphides do suffer from various drawbacks such as recombination, toxicity, low photoresponse. To overcome these drawbacks, many attempts have been made to modify the properties of metal sulphides. These include doping, coupling with highly effective and low toxic metal sulphides, loading of noble metals, shape control, crystal defect engineering, sensitization, doping and formation of heterojunctions or composite catalysts. Table 1 shows some photocatalysts based on metal sulphide materials with their photocatalytic applications.

Metal nitrides, oxynitrides, non-metal-nitrides

Metal nitrides and oxynitrides have found their role mainly in photocatalytic and photoelectrocatalytic hydrogen production via water splitting and other ways. For the conversion of light energy into sufficient chemical energy, the photocatalytic water splitting into hydrogen and oxygen has been explored in recent years. It is one of the greener approaches and has attained attention for potential large-scale use of

Table 1 Metal sulphide-based photocatalysts with their photocatalytic performances

S. no.	Photocatalyst	Light source	Photocatalytic application	References
1.	CdS	Visible light	Overall water splitting	Shangguan and Yoshida (2002)
2.	$ZnIn_2S_4$	> 420	Hydrogen production	Shen et al. (2009)
3.	$AgGaS_2$	> 420	Hydrogen production	Jang et al. (2007)
4.	CdS/CNT	> 400		Kim and Park (2011)
5.	Cu-doped ZnS	Overall spectrum	Overall water splitting process	Arai et al. (2008)
6.	CdS	Ultraviolet	Water disinfection treatment	Sathish et al. (2006)
7.	CdS/alumina	Overall spectrum		Sinha et al. (2001)
8.	NiS_2	Visible light	Hydrogen production	Song et al. (2016)
9.	Cr_2S_3	Sunlight	Dye degradation	Hussain et al. (2017)
10.	Bi_2S_3	UV light	Methylene blue removal	Helal et al. (2016)

The sulphides suffer from various drawbacks which are overcome by doping and formation of composites

solar energy. Keeping band gap, band positions and photocarrier mobility properties in mind, the designing of novel or effective photocatalysts like metal nitrides/oxynitrides has been done (Takata et al. 2015). N-doping path has been used for many semiconductor oxides so as to capture visible active. Different groups worked for the preparation of zinc oxynitrides powder or thin films (Li and Haneda 2003). In the photodecomposition of acetaldehyde in the visible region, the photocatalytic activity of N-doped ZnO increased dramatically. But no such improvement was observed while using UV light. The hydrolysis of ZnO can be done by raising the nitrogen concentration without lowering the stability of the material. Many other approaches also combine the N-doped ZnO properties with other semiconductor metal oxides. Therefore, for the study of photocatalytic deterioration of acetaldehyde, MO_X (M = Fe, W, V, Ce) have been studied. By adding V_2O_5 and WO_3, the photocatalytic activity in the visible light of N-containing ZnO samples was enhanced (Li et al. 2004, 2005a). There are some nitride/oxynitrides photocatalysts used for water splitting through visible light. This is done because these oxynitrides avoid photodissociation which is not possible in metal oxides and had a good band gap. It is a fact that the 2*p* orbital of N possess a higher potential energy than 2*p* orbital of oxygen, which indicates that metal nitrides and oxynitrides may be promising photocatalysts. If the cationic components are not changed, then conduction band levels will not significantly be affected (Fang et al. 2001). As N^{3-} and O^{2-} have similar ionic radius, the half or full substitution of N^{3-} for full or part of O^{2-} in the oxide is possible in some cases.

Among nitrides and oxynitrides, boron nitride (BN) (Liu et al. 2017b), Si_3N_4 (Yang et al. 2018), GaON (Cheng et al. 2017), AlON (Du et al. 2015), Ga–Zn oxynitride (Adeli and Taghipour 2016), Ga–In–Zn oxynitride (Kamata et al. 2009) and $LaTiO_2N$ (Kasahara et al. 2003) have been found to be good photocatalysts. For synthesis of metal oxynitrides, nitridation of metal oxides in a NH_3 flow is the most common methodology adopted. Ammonia decomposes on heating and formation of NH and NH_2 radicals which abstract O from oxide and N is introduced. It was shown that when the nitridation occurs at mild conditions (ammonia flow rate—20 mL min^{-1}, *T*—1123 K, duration—15 h). TaON is formed. But if NH_3 flow is raised to 500 mL min^{-1}, Ta_3N_5 is formed (Stampfl and Freeman 2005). In the nitridation process, the homogeneity is a major issue to be addressed. So for nitridation of oxide as homogeneously as possible, nitridation should be repeated with grinding and mixing halfway. In addition, uniform NH_3 flow should be ensured by reducing a single nitride metal oxide and swathing it in fibrous materials as silica wool (Logvinovich et al. 2010). Most of the transition metal oxynitrides are thermally less stable (even at 100 K), so the decomposition temperature can be increased by high-pressure environment of N_2 or NH_3. In addition for producing high-quality nitrides, flux method is used which is a single-crystal growth method. In this method, inorganic materials or metals with a high melting point (called flux) are used as solvents. The precursor is used as solute and then crystals are grown from solution which is oversaturated by either decrease in temperature or lowering the solubility.

There is only limited choice of photocatalysis such as Ta_3N_5, TaON or many other material of oxynitrides family which are used for overall water splitting. Ta_3N_5 is a captivating photocatalyst with extended visible absorption (600 nm) and good ability for redox reaction which theoretically achieve the solar energy to hydrogen conversion efficiency of ~ 17%. It has good stability under illumination and under photocatalytic reaction condition (Nurlaela et al. 2016). For the overall water splitting, the first metal nitride photocatalysts which has been found is Ge_3N_4. Ge_3N_4 is also known to be polymorphic, having α, β, *Y* and *d* phases, and these phases have different structures. The β phase is better when combined with a suitable co-catalyst and is used for overall water splitting purpose (Takata et al. 2015).

Tantalum nitride (Ta_3N_5) has an orthorhombic structure and is one of the most common photocatalyst employed for water splitting. It generates hydrogen from water by absorbing light up to 600 nm. Watanabe and co-workers showed that thermal treatment under high NH_3 pressure can enhance the H_2 production from methanol using Ta_3N_5. The treatment temperature was set at 823 K, and duration was 24 h with pressure variation from 10 to 100 MPa. When such treatment was done, the absorption was increased over 600 nm. The hydrogen production activity was enhanced (Yungi et al. 2006). Du et al. synthesized aluminium oxynitride (AlON) by a carbothermal reduction and nitridation method. AlON catalyst possessed a band gap of 5.2 eV with more of UV absorption. The catalyst was used for photodegradation of methyl orange dye under UV light irradiation (Du et al. 2015).

In another work, zinc-doped gallium oxynitride nanowires enriched with surface defects are fabricated via simple electrospinning and controlled calcination process under ammonia atmosphere. The catalysts were used for degradation of rhodamine B dye under visible light. The structure analysis of zinc-doped GaON showed that the surface oxygen vacancies were responsible for the high quantum efficiency (Cheng et al. 2017). Next photocatalyst of interest is lanthanum titanium oxynitride ($LaTiO_2N$). This is abundant, non-toxic and inexpensive as compared to tantalum compounds. This also has hydrogen-producing capacity from water under visible exposure. $LaTiO_2N$ is generally synthesized by nitridation of either $La_2Ti_2O_7$ or $LaTiO_{3.5}$ which is a ferroelectric material. The precursor $La_2Ti_2O_7$ is synthesized by a solid-state reaction between La_2O_3 and TiO_2. Perovskites oxynitrides are another category of photocatalysts. $LaMO_2N$ (M = Ti, Zr), $LaMON_2$ (M = Nb, Ta)

are well-known oxynitrides which absorb near 600 nm (Ebbinghaus et al. 2009).

Perovskite oxynitrides can be synthesized by conventional nitridation technique where precursor is a metal oxide or mixture of metal, or where an oxide precursor and carbonate is thermally treated under NH_3 flow. Zhang et al. prepared lanthanum tantalum oxynitride ($LaTaON_2$) powders by one-step flux method and utilized for photoelectrochemical water splitting. Under visible light, hydrogen was produced on the surface of Pt-$LaTaON_2$ which shows the catalytic activity for H_2 evolution (Zhang et al. 2014b). Among non-metal nitrides, silicon nitride (Si_3N_4) has attracted attention with a wide band gap of ~ 5 eV. It has high stability, strength and low density. However, poor visible response limits its use which is generally overcome by doping and formation of composite catalysts or heterojunctions with low band gap semiconductors. Hexagonal boron nitride (BN) is a two-dimensional crystalline material which has similar structure to graphene (so-called white graphene). It possesses a wide band gap, high chemical and thermal stability, conductivity and large surface area (Lei et al. 2013). BN is not generally considered as a catalyst, but it is mostly used as a semiconductor in coupled form or used as a catalytic support because of its intrinsic properties. However, boron nitride-based materials have been used as catalysts in removal of organic pollutants (Wang et al. 2011), metal reduction (Xu et al. 2017) and hydrogen production (Huang et al. 2015). Table 2 shows various metal nitrides and oxynitrides for photocatalytic applications.

Metal phosphides and black phosphorous

Phosphorus (P) is one of the most abundant elements on earth (Zhu et al. 2018) with several allotropes as red, black and white. Black phosphorous has gained interest since it was first used in field-effect transistors. It has a tuneable band gap of (~ 0.3 eV to ~ 2.1 eV) and is functional in near-infrared region (Buscema et al. 2014). But because of low band gap, black phosphorous suffers from the drawback of high recombination of electron–hole pairs. So in general, it is utilized as a co-catalyst or a part of composite catalyst or heterostructures. Zhu and co-workers synthesized 2-D hybrids of black phosphorous/WS_2 for NIR hydrogen production. They observed that the rate was 21- and 50-fold higher than pure phosphorous and WS_2 (Zhu et al. 2018). In another work, metal-free photocatalyst–black phosphorous decorated with g-C_3N_4 nanosheets was prepared for Cr(VI) photoreduction and nitrogen photofixation under visible irradiation. A nitrogen conversion of 347.5 μmol L^{-1} h^{-1} was obtained. The increased high charge carrier separation was due to the formation of C–P covalent bonds (Qiu et al. 2018).

Among phosphides, transition metal phosphides possess high stability and activity in addition to the abundance. In comparison with nitrides and sulphides, metal phosphides have been found to perform well for catalytic applications such as oxidation–reduction, aromatization, hydrogenolysis. Many routes have been involved for the preparation of transition metal phosphides. There include reduction of metal phosphines or phosphates by temperature-programmed reduction method (Lee and Oyama 2006). By conducting a reaction of amorphous Ni–B alloy with PH_3, the Ni_2P catalyst has been prepared. This catalyst has good catalytic activity in hydrodisulfurization of dibenzothiophene and is used for the synthesis of other metal phosphides like CoP, Cu_3P, FeP and so on. Hydrodisulfurization of crude oil fractions is done by many phosphides, but Ni_2P has good photocatalytic activity (Clark and Oyama 2003). Figure 3 shows the various phosphides used for photocatalytic applications in environmental treatment. These include phosphides of representative, transition metal, rare earth elements and the combinations.

For the integration of extent and supported CoP, Ni_2P, FeP, Cu_3P catalysts, the following method is used. Firstly

Table 2 Utilization of metal nitrides and oxynitrides and non-metal nitrides as photocatalysts for various environmental applications

S. no.	Photocatalyst	Light source	Photocatalytic application	References
1.	TaON	Visible	Photo-Fenton degradation of Atrazine	Du et al. (2011)
2.	InGaN	Visible	Hydrogen production	Chowdhury et al. (2015)
3.	$LaTiO_2N$	Visible	Hydrogen generation	Li et al. (2015b)
4.	Ta_3N_5	Overall spectrum	Overall water splitting process	Yuliati et al. (2010)
5.	GaN/ZnS	Solar	Water splitting	Hassan et al. (2018)
6.	Si_3N_4	UV–visible	Degradation of tetracycline	Yang et al. (2018)
7.	Boron carbon nitride	UV light	Degradation of Cibacron Yellow FN-2R dye	Sivaprakash et al. (2018)
8.	BN/CN	$\lambda > 305$ nm	Hydrogen production	He et al. (2017)
9.	Zinc-doped GaON	Visible	Degradation of rhodamine B	Cheng et al. (2017)
10.	$SrNbO_2N$	Visible	Hydrogen evolution	Wang et al. (2015a)

Among non-metal nitrides, carbon nitride and boron nitride have been most successful in photocatalysis

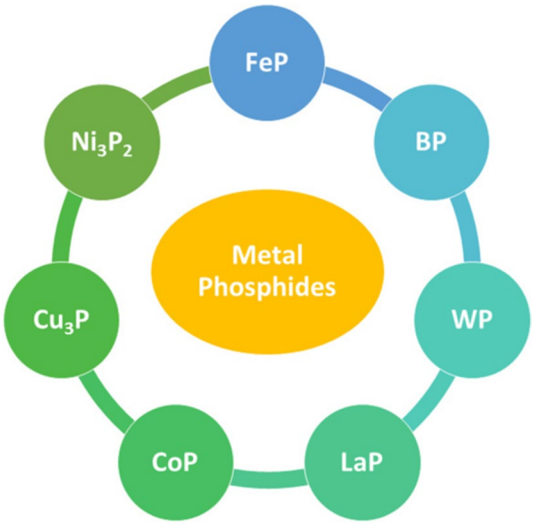

Fig. 3 Various metal phosphides as candidates for photocatalytic applications in environmental treatment. These include phosphides of representative elements, transition metals and rare earth metals

metal pyrophosphates precursors ($Ni_2P_2O_7$, $Fe_2P_2O_7$) were prepared under intense stirring by mixing the stochiometric amounts of potassium pyrophosphates ($K_4P_2O_7{\cdot}3H_2O$) and metal chlorides ($NiCl_2{\cdot}6H_2O$, $CuCl{\cdot}2H_2O$. Metal pyrophosphate was placed in tubular reactor and heated at 700 °C in flowing H_2. The reaction proceeds for 7 h. Finally, the silicon dioxide supported Ni_2P were introduced in SiO_2 impregnation. The precursors were preserved at 80 °C for 3 h in vacuum oven (Zhang et al. 2014c).

Metal phosphides like MoP, WP and Fe_2P were used for the study of hydro-treatment reactions. Due to high reactivity, the metal phosphides like MoP, Ni_2P and WP catalysts are greatly used. But not much attention is given to Fe_2P because of its poor activity in hydro-treatment reactions. The preparation of metal phosphides includes two steps: in the first step by combining stoichiometric quantities of metal salt phosphate precursors are prepared. In the next step, the phosphate precursors are transformed into phosphides according to temperature-programmed reduction procedure as described by Prins and co-workers (Yao et al. 2016). Solvothermal method is used for synthesizing metal sulphides using organic solvents as reaction medium. The morphology and shape can be controlled by solvothermal process. In a work by Callejas et al., iron phosphide was synthesized successfully by this method (Callejas et al. 2014). $Fe(CO)_5$ was heated with oleylamine and 1-octadecene at 190 °C to form Fe nanoparticles. The Fe nanoparticles were than treated with trioctylphosphine at 340 °C for 1 h to form FeP. The synthesis can also be performed by solid-state phase reaction. Li and co-workers synthesized a series of Ni_xP_y catalysts by solid-state reaction of $Ni(OH)_2$ and NaH_2PO_2 with a molar ratio of 1:5 in an argon atmosphere (Li et al. 2016a). O'brien group synthesized single-crystalline CoP nanowires with one-pot metal–organic method (Li et al. 2005b), while polycrystalline form was synthesized by solvothermal route (Hou et al. 2005). In a work by Mi and group, nickel phosphide was synthesized by solvothermal method at 180 °C. Nickel chloride and white phosphorous and sodium dodecylbenzene sulphonate were used as precursors. $Ni_{12}P_5$ was obtained in ethanol solution, while pure Ni_2P was formed in mixed solvent water/ethanol (10:10) (Mi et al. 2011).

In a similar fashion, Co_2P was synthesized using cobalt dichloride and white phosphorous as reactants and ethanol/water mixture as solvent. Urchin-like Co_2P structures were formed and were used for the degradation of dyes (Ni et al. 2009). Boron nitride-decorated zinc phosphide nanowires were prepared successfully. The Zn_3P_2 nanowires were synthesized by chemical vapour deposition method. Photocatalytic potential was tested by studying the visible-assisted water disinfection by inactivation of *E. coli* (Vance et al. 2018). Among phosphides of rare earth metals, indium phosphide has been explored the most and used in electronics and high-speed communications. This is because of its good conductivity and metalloid nature (Yin et al. 2004). However, the photocatalytic activity has been studied by very few groups. There are several methods reported for synthesis of InP nanoparticles as laser, solution phase and chemical vapour deposition. In general, the indium and phosphide precursors (metal organic materials) were used for growth of InP. But these materials are quite toxic. So the solution phase methodology is the preferred one as it is facile route and also parameters can be easily controlled. Yu and group synthesized InP nanoneedles and nanotubes by solvothermal route. They reported that there was blueshift in nanoform as compared to the bulk form. The photocatalytic efficiency was tested for degradation of rhodamine B dye (Yu et al. 2017a). Cost-effective and less toxic metal-free photocatalysts have been explored but not fully exploited. Photocatalysts based on graphene, carbon nitride, boron phosphide, boron nitride, $C_3N_3S_3$, boron carbon oxy nitride, etc., containing elements C, N, B, S, have demonstrated to perform in photocatalytic applications. So considering such phosphide-based metal-free catalysts, Boron phosphide is an interesting candidate. Boron phosphide (BP) is an important photocatalyst as it is composed of boron and phosphorous which are lightweight and abundant elements. In addition, it is a transition metal-free catalyst. BP is thermally stable and resistant to chemical attack. BP is a semiconductor with a band gap of ~ 2.0 eV. BP can be doped to form both *n*-type (excess P doping) and *p*-type semiconductors (excess B doping). However, *n*-type has higher conductivity. *n*-type BP was synthesized by a solid-state route and was found to be extremely stable under acid or alkali attack. It was reported that BP performed excellent for visible light-powered H_2 production even without noble metals as co-catalyst (Shi

et al. 2016). Table 3 shows various phosphides employed as photocatalysts.

Metal oxyhalides and halides

For the energy harvesting and environment remediation, many photocatalysts depending on nanomaterials have been investigated. Oxyhalide-based photocatalysts mainly include bismuth oxy halides such as BiOBr, BiOCl, BiOF and BiOI. The halides as catalysts include mainly silver based, i.e. AgCl, AgBr and AgI. Bismuth oxyhalides (BiOX) present a new interesting class of materials with a layered structure for energy conversion and environment remediation. They belong to family of main group of multi-component metal halides. As Cl, Br and I belong to same group so BiOCl, BiOBr and BiOI possess the similar properties. Unlike metal oxides TiO_2 and ZnO, BiOX possesses variable band gap as 1.8 eV for BiOI, 2.8 eV for BiOBr and nearly 3.5 eV for BiOCl. In addition, various synthetic strategies lead to formation of BiOX in the form of nanorods, nanoflowers, nanobelts, nanosheets, nanoplates, thin films, etc., with different surface morphology, specific surface area and optical band gaps. For utilization of BiOX in industrial and environmental applications, various attempts have been made by various research groups for increasing the spectrum capture, decreasing the recombination and boosting the charge transfer.

The main approaches or synthetic routes for BiOX include hydrothermal, solvothermal, sonochemical, microwave, precipitation, emulsion and template method. However, for preparation of hybrid catalysts based on oxyhalides combination of these with other techniques as chemical vapour deposition can also be involved. Usually, bismuth oxyhalides tend to form a 2-dimensional layered crystalline structure, and for formation of 3-dimensional material, assembling of 2-dimensional nanosheets forming a hollow structure is required.

BIOBr nanosheets were prepared with (001) facet domination. These were utilized for photocatalytic reduction of CO_2 under simulated sunlight. A CO production of 4.45 μmol h^{-1} g^{-1} was achieved because of high surface area, lower recombination and high reduction ability (Wu et al. 2017). With the help of these properties, they have photocatalytic applications for energy harvesting and environment remediation (Li et al. 2014). The layered BiOX semiconductor materials have a tetragonal PbFCl-breed arrangement. This structure consists of [X–Bi–O–Bi–X] slices deformed together by non-bonding interactions through halogen atoms. The halogen layers are stacked by non-bonding forces and interactions within $[Bi_2O_2]$ emerge from covalent bonds. The bismuth oxyhalides have suitable band structure which helps in absorbing sunlight so that photocatalytic action reaction can be initiated. But due to the mismatch between the light harvesting and band gap, poor selectivity and less activity sites their applications are limited (Zhang et al. 2006). The strong interlayer covalent bonding and weak interlayer van der Waals interaction in BiOX structure give rise to highly anisotropic, electrical, optical and mechanical properties which makes BiOX suitable for photocatalytic waste water and particular oxidation of alcohol (Guan et al. 2013; Xu et al. 2011).

For the elimination of aqueous dyes under UV irradiation, good results have been obtained with bismuth oxyhalides. BiOCl has a layered tetragonal structure and has wide band gap which is higher than that of TiO_2. Zhang et al. synthesized BiOCl powders by the help of acid hydrolysis of Bi_2O_3 in excess of HCl. MO degradation under UV light having photocatalytic activity was compared with TiO_2-P25 (Zhang et al. 2006). Because of BiOCl presence, the MO disappears fast and this activity was done in two successive

Table 3 Phosphorous- and phosphide-based photocatalysts for environmental applications

	Photocatalyst	Light source	Application	References
1.	Black phosphorous nanoflakes	Near-infrared	Hydrogen evolution	Lee et al. (2016)
2.	Black phosphorous/WS_2	> 780 nm	Photocatalytic hydrogen production	Zhu et al. (2018)
3.	Black phosphorous/g-C_3N_4	Visible light	Photoreduction of Cr(VI) and photofixation of N_2	Qiu et al. (2018)
4.	InP	UV light	Degradation of rhodamine B	Yu et al. (2017a)
5.	Zn_3P_2	Visible light	Photokilling of *E. coli*	Vance et al. (2018)
6.	Boron phosphide	Visible light	Hydrogen evolution	Shi et al. (2016)
7.	$Ni_{12}P_5$	UV light	Safranine T and pyronine B removal	Li et al. (2009b)
8.	Co_xP/CdS	Visible light	Hydrogen generation	Dong et al. (2017b)
9.	Fe_2P/CdS	Visible light	Hydrogen generation	Pan et al. (2018)
10.	Co_2P	UV light (365 nm)	Degradation of pyronine B and fluorescein dyes	Ni et al. (2009)
11.	WP-loaded CdS	Visible light	Hydrogen production	Zhang et al. (2017a)
12.	NiCoP	Visible light	Hydrogen evolution	Song and Zhang (2018)

In addition to photocatalysis, sulphides have found role in organic transformation reactions too

runs. The photocatalytic removal of RhB was performed over Bi_2O_3 and BiOCl nanofibres obtained by electrospinning. The obtained BiOCl has band gap energy of about 3.2 eV. The immense photocatalytic activity of BiOCl comes from delocalization of minimum conduction band, and high mobility to the photogenerated charges is granted by Bi 6*p* orbitals (Wang et al. 2008). Other than degradation of dyes, the BiOCl had also shown photocatalytic activity towards degradation of isopropanol.

Yb^{3+}-doped BiOI photocatalyst was prepared by a facile hydrothermal method. 2% Yb^{3+}-doped BiOI showed highest degradation of rhodamine B dye, which was 2 times the bare BiOI. In addition, the catalyst exhibited high photodegradation of herbicide isoproturon (Zhang et al. 2018b). In order to improve the photocatalytic activity of halides and oxyhalides, heterojunctions or composite catalysts are formed. Formation of heterojunctions is the most common methodology for improving the catalytic efficiency of a semiconductor and separation of photo-induced charge carriers. Recently, g-C_3N_4/BiOCl heterojunction was synthesized where nano-g-C_3N_4 was loaded in exposed facets (001) and (010) of BiOCl. The electrons transferring from carbon nitride to BiOCl have a longer time for exposed face (001) than for (010) (Li et al. 2015a). The two samples displayed different activity for degradation of methyl orange and phenol. This infers that exposing of facets in semiconductors can be an effective strategy for higher photoactivity.

A visible active photocatalyst AgI/g-C_3N_4 was synthesized by deposition–precipitation method. The composite catalyst was utilized for degradation of antibiotic diclofenac under visible light. The rate constant reached 0.561 min^{-1} when the molar mass ratio of AgI was 45% which 12.5 and 43.2 times higher than AgI and gC_3N_4, respectively (Zhang et al. 2017b). Similar other junctions were formed utilizing halides and oxyhalides for a better performance. Table 4 shows some of halides and heterojunctions for environmental applications.

Ferrites as Magnetically Recoverable Photocatalysts

In recent years, recovery and reusability of photocatalysts have been a major issue. In this regard, various suitable modifications of photocatalysts have been performed. One of them is introduction of magnetic photocatalysts. Magnetic nanoparticles have grabbed considerable interest due to their super-paramagnetic and ferromagnetic properties, high adsorption capacity and bio-compatibility. Particularly transition metal ferrites are the most important candidates. They are classified as spinel (MFe_2O_4), garnet ($M_3Fe_5O_{12}$), orthoferrite ($MFeO_3$) and hexaferrite ($SrFe_{12}O_{19}$ and $BaFe_{12}O_{19}$) (Kefeni et al. 2017). Among all these, spinel ferrites have been studied extensively for adsorptional and photocatalytic applications, especially in wastewater treatment.

For synthesis of spinel ferrites, two broad approaches are involved—bottom-up and top-down. The bottom-up options include hydrothermal, solvothermal, co-precipitation, microwave, gel-combustion and sonochemical. In hydrothermal method, generally $FeCl_3{\cdot}6H_2O$ or $Fe(NO_3)_3{\cdot}9H_2O$ and a salt of metal are dissolved in water with neutral to alkaline pH. The mixture is then thermally treated at high temperature and cooled at room temperature. The material is collected by filtration or centrifugation. In the sol–gel process and gel-combustion method, solution of metal salt and citric acid is mixed to form a gel in water or ethanol. The homogenized gel is dried and sintered at varying temperatures (specific to each ferrite) for different times. In the co-precipitation technique, the metal salt and Fe(III) salt are dissolved in water and surfactant is added. In a neutral-to-alkaline pH solution, gentle heating is provided to precipitate the ferrite. A lot of structural

Table 4 Halides, oxyhalide-based photocatalysts for environmental photocatalytic applications

S. no.	Photocatalyst	Synthetic method	Photocatalytic performance	References
1.	BiOCl	Hydrothermal route	Degradation of RhB	Cai et al. (2018)
2.	BiOI	Solvothermal route	Degradation of gallic acid	Mera et al. (2017)
3.	Iodide modified $Bi_4O_5Br_2$	Alcoholysis–hydrolysis method	Degradation of BPA and NO	Li et al. (2018b)
4.	BiOF	PVA-assisted hydrothermal method	Degradation of MO	Yang et al. (2017)
5.	AgBr	Emulsion method	Hydrogen evolution	Kobayashi et al. (2014)
6.	AgCl	Hydrothermal	Degradation of MO	Guo et al. (2017)
7.	$AgI/AgIO_3$	Mild ion exchange	Removal of RhB	Cao et al. (2016)
8.	Bi@BiOCl	Hydrothermal	Removal of RhB	Ye et al. (2012)
9.	Mn@BiOCl	Hydrothermal	Photodegradation of RhB	Zhao et al. (2016a)
10.	$AgCl/Ag_2S$	One-pot hydrothermal method	Photodegradation of MO	Zarghami et al. (2016)

Bismuth halides and oxy halides have been the most popular and effective with wide range of optical performance

PVA polyvinyl alcohol, *BPA* bisphenol A, *RhB* Rhodamine B, *MO* methyl orange

changes can be observed with doping concentrations and dopants in ferrites which make them ideal for tuning (Kane et al. 2018; Raghuvanshi et al. 2018; Satalkar et al. 2018; Tatarchuk et al. 2017).

There are various applications of photocatalysis in various fields, like purification of contaminants from water (Kumar et al. 2014). Calcium ferrite ($CaFe_2O_4$) has been used for effective reduction of CO_2 into methanol and other products. Ferrites possess high adsorbing power which makes them ideal candidates in photocatalytic applications used for environment decontamination. The semiconductor properties of photocatalyst make it very useful for the deterioration of organic contaminants which is helpful for the remediation of hazardous waste and polluted ground water and also has control on toxic air pollutants (Sharma et al. 2017b). The use of spinel $ZnFe_2O_4$ in photocatalysis has great advantage as it has covetable optical absorption with precise band gap of ~ 1.9 eV and low-cost excellent photochemical stability (Sun et al. 2012). This photocatalyst was used for the debasement of many dyes like methyl orange under UV radiation, methylene blue under real sunlight irradiation or visible light irradiation (Xie et al. 2013), Procion Red dye in the existence of H_2O_2/visible radiation (Anchieta et al. 2014). Magnetically recoverable zinc ferrite ($ZnFe_2O_4$) was synthesized by molten salt method and utilized for degradation of rhodamine B dye under UV irradiation (98% degradation) (Preethi et al. 2017).

Many nanostructured zinc ferrite-type essentials $Zn_XFe_{3-x}O_4$ ($X = 0.25, 1, 0.5$) having average crystallite size were prepared by mechanic-chemical treatment co-precipitation. These zinc ferrite-type materials are used for the photocatalytic removal of malachite green dye in UV light. Optical absorption for the narrow band gap, excellent photochemical stability, electronic structure, low cost and strong magnetism are some advantages of using spinel $ZnFe_2O_4$ in photocatalysis (Sun et al. 2012).

Cobalt ferrite ($CoFe_2O_4$) as an excellent magnetic photocatalyst is used in biomedical, recording technology and electronics. The arrangement of spinel ferrite is in two different sites and depends on distribution of divalent ions (Co^{2+}) and trivalent ions (Fe^{3+}). When cobalt ion is replaced to cobalt ferrite having different divalent ions, it leads to different properties and useful applications. The physiochemical properties are enhanced by substituting various cations in cobalt ferrite (Mane et al. 2011). Copper-substituted cobalt ferrite having photocatalytic activity has the applications in degradation of dyes and antibacterial action (Mishra et al. 2012).

There is another ferrite photocatalysts, i.e. magnesium ferrite photocatalysts, which is used for the photoanalysis of methylene blue, and is an industrial level dye. This photocatalysis is synthesized with the help of solid–solid method in Mg:Fe ratio 1:2 by mol. Magnesium ferrite ($MgFe_2O_4$) is ferrite-based photocatalysts which has its support in both acidic basic medium and resistant and towards photocorrosion. It is non-poisonous and having good photochemical as well as chemical stability. It has less sensitivity towards photoanodic corrosion and has small band gap (Batista et al. 2010). Because of small band gap and less sensitivity towards photoanodic corrosion, the magnesium ferrite in its spinel structure can absorb visible light at about 2.0 eV (Kim et al. 2009). This material has number of applications like magnetic heterogeneous catalysis, sensors and also in magnetic technologies (Maensiri et al. 2009). Table 5 shows various ferrites and combinations as magnetically recoverable photocatalysts for various environmental applications.

Carbon-based photocatalysts

The heart of the advanced oxidation processes via semiconductor photocatalysis is the energy conversion by the photocatalyst. Thus, tremendous effort is laid down on the

Table 5 Utilization of ferrites as magnetically recoverable photocatalysts under visible and solar light

S. no.	Photocatalyst	Synthetic method	Photocatalytic performance	References
1.	$ZnFe_2O4$	Sol–gel	Photoreduction of Cr(VI) (60% reduction in 3 h)	Rekhila et al. (2016)
2.	$CoFe_2O_4$/Graphene	Combustion method	Photodegradation of MB d (~ 100% removal in 2 h)	Zhang et al. (2013)
3.	$CoFe_2O_4$/AgBr	Precipitation	Removal of 95% MO and 92% RhB removal in 20 min	Li et al. (2017c)
4.	Ag@$NiFe_2O_4$	Combustion method	Removal of MB (~ 100% in 2 h)	Zhang et al. (2014a)
5.	$NiFe_2O_4/Bi_2O_3$	Hydrothermal	Removal of TCL (90.78% removal in 1.5 h)	Ren et al. (2014)
6.	$CuFe_2O_4@C_3N_4$	Precipitation	Removal of Orange II dye (98% removal in 210 min)	Yao et al. (2015)
7.	$CuFe_2O_4$	Sol–gel	H_2 production (1.72 mmol g^{-1} h^{-1})	Yang et al. (2009)
8.	$NiFe_2O_4$	Hydrothermal	Decomposition of CO_2 into C and O_2 (90%)	Lin et al. (2011)
9.	$Mn_{(1-x)}Mg_xFe_2O_4$ ($x = 0$–0.7)	Microwave-assisted co-precipitation	Removal of MB (69.5% removal in 2 h)	Attia et al. (2017)
10.	$ZnSm_xFe_{2-x}O_4$	Co-precipitation	Removal of MO (~ 100% removal in 80 min)	Rashmi et al. (2017)

MB methylene blue, *TCL* tetracycline

designing and production of highly efficient photocatalysts. In recent years, carbon-based metal-free photocatalysts have emerged as alternative class because of their attractive properties as tuneable band gap, high surface area, abundance and low toxicity. These include photocatalysts based on B, C, N, S, Se, P and carbon-based materials as graphene oxide, reduced graphene oxide, carbon quantum dots, organic conducting polymers and graphitic carbon nitride (g-C_3N_4). Conducting polymers as polyaniline have been utilized for water purification by incorporating into hydrogels (Sharma et al. 2015) and combining with metal oxides (Kant et al. 2013). These polymers possess high conductivity, stability and facilitate separation and generation of charge carriers like semiconductors. Graphene oxide (GO) has been used as a promoter in the photocatalytic reactions. It has received attention because of its structural similarity to graphene and is open to modification as introduction of hydroxyl and carboxyl groups in various nanocomposites. The major structural difference is that the surface of GO has a lot of oxygen-containing groups, such as COOH, OH, C=O, etc. which increases its adsorption or loading potential (Dong et al. 2017a). However, GO is generally converted into reduced graphene oxide (RGO) during the synthesis process. Most of the nanocomposite catalysts include RGO only. The introduction of GO/RGO into the catalyst reduces the electron–hole recombination and increases in reactive sites and high absorption. It is widely used in different interactions as hydrogen bonding and electrostatic interactions in hydrogels.

Graphitic carbon nitride (g-C_3N_4) has emerged out to be fascinating alternative to conventional photocatalysts. However, the discovery of polymeric carbon nitride goes long back in 1834 by Berzelius. It is a visible light photocatalyst, having two-dimensional structure, good chemical stability and tuneable electronic structure (Zhao et al. 2015). Graphitic carbon nitride is the most stable allotrope of polymeric carbon nitride. It consists of s-triazine units. As the s-triazine ring (C_3N_3) has aromatic character, these units tend to form a 2-dimensional polymer like graphite. The thermal studies of g-C_3N_4 reveal that is stable even at 600 °C. The conventional g-C_3N_4 shows absorption at ~ 420 nm; however, this shifts according to precursor and the methodology adopted to prepare.

The g-C_3N_4 is present in abundance and easily synthesized via one-step polymerization of cheap feedstock such as cyanamide (Wang et al. 2009), melamine (Yan et al. 2010), urea (Liu et al. 2012) and dicyandiamide (Zhang et al. 2012). Porous oxygen-doped graphitic carbon nitride nanosheets were synthesized by thermal polymerization of using urea and sodium oleate. The surface are of various compositions varied from 57.3 to 111.9 $m^2\ g^{-1}$. According to the dopant percentage, the band gaps varied from 2.63 to 2.82 eV, thus facilitating the visible absorption (Chen et al. 2017). The sodium nitrate treatment has been done to alter the surface morphology. All the modified g-C_3N_4 samples had a visible absorption to different extents. The high viable absorption intensity of modified g-C_3N_4 was attributed to modification by sodium nitrate. The samples were used for photocatalytic degradation for tylosin. Table 6 shows the

Table 6 Carbon-based photocatalysts, their precursors and photocatalytic applications

S. no.	Catalyst	Precursors	Photocatalytic applications	References
1.	g-C_3N_4	Cyanamide	H_2 production	Wang et al. (2009)
2.	Amorphous g-C_3N_4	Dicyandiamide	H_2 production	Kang et al. (2015)
3.	3D-porous g-C_3N_4	Melamine	Removal of organic pollutants	Yuan et al. (2016)
4.	g-C_3N_4	Cyanamide	H_2O_2 production	Shiraishi et al. (2014)
5.	Porous g-C_3N_4	Removal	Removal of organic pollutants	Kumar et al. (2018c), Xiao et al. (2016)
6.	Nitrogen-rich g-C_3N_4	Melamine	Removal of CV	Dillip et al. (2017)
7.	Graphene quantum dots modified g-C_3N_4	Urea, graphite and pyrene	Removal of Rh B	Liu et al. (2017c)
8.	g-C_3N_4/GO aerogel	Graphite powder and urea	Removal of MO, MB and bromate	Tang et al. (2017)
9.	$C_3N_3S_3$/RGO	Graphite and thiocyanic acid	Removal of benzylic alcohols	Xu et al. (2014)
10.	Polydopamine/g-C_3N_4	Dopamine hydrochloride and melamine	Removal of MB, Rh B and phenol	Yu et al. (2017b)
11.	Folded nanoporous g-C_3N_4	Urea	Removal of MB	Li et al. (2017b)
12.	g-C_3N_4-CNTs	Urea and carbon nanotubes	H_2 production	Zhao et al. (2018a)
13.	Conjugate Polyene/g-C_3N_4	Urea and Polyvinyl alcohol	H_2 production	Li et al. (2018a)
14.	Anthraquinone/g-C_3N_4	Melamine	H_2 production	Kim et al. (2018)
15.	Graphitic carbon/carbon nitride	Melamine and sucrose	H_2 production	An et al. (2017)

CV crystal violet

various carbon-based photocatalysts, their precursors and the photocatalytic application for which they are employed. Polydopamine/graphitic carbon nitride (PDA/g-C_3N_4) was synthesized by polymerization of dopamine onto surface of g-C_3N_4. 10%PDA/g-C_3N_4 was found to degrade 98% of methylene blue in 3 h. It was reported that PDA accepts electrons from semiconductor g-C_3N_4 and thus reduces recombination (Yu et al. 2017b). Lu et al. synthesized carbon and graphitic carbon nitride composites (C/CN) by a one-pot method using hydroxyl methylated melamine as template. The composite was used for visible powered degradation of methylene blue dye, and rate constant was 1.9 times for that of pure CN (Lu et al. 2018b). As an innovation, a novel graphitic carbon nitride photocatalyst was prepared by a facile one-pot thermo-induced copolymerization method using urea and tetracyanoethylene as precursors (Wang et al. 2018d). The catalysts were used for degradation of Orange II dye under visible irradiation with a 91% removal in 60 min. Ding and group designed a photocatalytic system based on g-C_3N_4 and mesoporous carbon for photocatalytic hydrogen evolution and photodegradation of methylene blue dye (Ding et al. 2018). A hydrogen evolution of 102 μmol h^{-1} was achieved, and the high charge separation efficiency was attributed to the presence of mesoporous carbon in the photocatalyst.

Xie et al. synthesized a surface charge modified g-C_3N_4 by protonation using nitric acid. Thus, they synthesized a 2D-2D type assembly of protonated carbon nitride (PCN) and graphene oxide, i.e. (PCN/RGO). Rhodamine B (RhB) and ciprofloxacin (CIP) were degraded under visible light with the highest efficiency for pCN/GO-5% (Xie et al. 2018). They assumed that the synergism of GO and PCN not only increased the interface area but also led to increased separation of the photogenerated charge carriers. Graphitic carbon nitride and graphene are used for hydrogels which are strong, stretchable and conducting. The photoactive hydrogels are a current area of interest (Sharma et al. 2018c). The hydrogel structure of a photocatalyst is beneficial as one gets the opportunity for improved loading, controllable reaction sites, increased strength, high surface area and high recyclability (Sharma et al. 2018a). In addition during in situ synthesis of photoactive hydrogel, the photoactive material can act as initiator for the polymerization reaction. Carbon nitride-based hydrogels were prepared by a facile route. The hydrogels possessed different shapes as cylindrical, sheet and tubular. The hydrogels were used for adsorptive removal of toxic dyes and photocatalytic hydrogen evolution. The H_2 production is less as compared to the powder form, but it could be improved by adjusting the configuration (i.e. thickness and structure). In addition to hydrogels, aerogels have also gained importance in recent years for environmental applications. Three-dimensional graphene-based aerogels have been utilized as photocatalysts with high solar spectrum capture because of their unique structure and properties. For synthesis of grapheme-based aerogels, graphene oxide (GO) is usually used as a precursor which can be hydrothermally converted into graphene and assembled into three-dimensional network with hydrogen bonding and π–π stacking. However, the electrical conductivity of GO is decreased considerably in an aerogel network. In a related work, commercial Elicarb graphene (EGR) was hybridized with GO to form a three-dimensional aerogel—Reduced graphene oxide@Elicarb Graphene-Eosin Y (RGO@EGR-EY). The aerogel with high electrical conductivity was utilized for visible-assisted photoreduction of Cr(VI). RGO@15%EGR-2EY aerogel reduced 98% of Cr(VI) in 20 min of visible exposure (Lu et al. 2018a). Similarly, many other carbon-based metal-free photocatalysts have been designed and synthesized. Some individual catalysts have limitations like low conductivity, which is generally overcome by hybridizing with other catalysts for a better performance. However, it may be the fact they have lower activity than metal-free catalysts, but their cost-effectiveness, abundance, high surface area, non-toxicity and bio-compatibility make them ideal.

Perovskite-based photocatalysts

Perovskite-based photocatalyst has a great interest in the area of photocatalysis. Perovskites are the class of compounds having general formula ABO_3 in which A site is engaged by larger cation and B site is engaged by smaller cation. Perovskites have many crystal structures varying from cubic (high symmetry) to triclinic (very low symmetry). Various solid-state reaction routes from oxides, hydrothermal, sol–gel, high-pressure techniques, vapour deposition methods have been utilized for the synthesis of perovskites. Different procedures can lead to formation of same perovskite but with different symmetries and even a different structure too. Ceramic route was the first technique used for the synthesis in which mixture of oxides was treated at high temperatures and processed later by ceramic powder methods.

Perovskite-based photocatalysts are $PbZrO_3$, $BaTiO_3$, $PbTiO_3$ and these are normally used piezoelectric compounds (Kanhere and Chen 2014). Multi-ferric behaviours is shown by $BiFeO_3$ thin films (Nuraje and Su 2013), whereas $SrTiO_3$ has excellent photocatalytic properties. Ag-modified lanthanum cobaltite ($LaCoO_3$) perovskite was prepared by hydrothermal route. The morphology analysis shows that the tetragonal shape of bare $LaCoO_3$ changes into square with incorporation of Ag. Ag–$LaCoO_3$ shows a good photocatalytic activity by degrading 99% of methylene blue dye (MB) in 10 min (Jayapandi et al. 2018). In a work by Dükkanc, $LaFeO_3$ perovskite was synthesized by sol–gel method by calcination at 500 °C. The catalyst was utilized for degradation of endocrine disruptor (BPA). The degradation was studied by using sonochemical, photocatalytic, Fenton

techniques and combination of these for getting insight into the effect of each onto degradation of BPA. Though $LaFeO_3$ shows a good photocatalytic activity, in this work it was found that it shows better results under sonochemical route (Dükkancı 2018).

Core–shell $SrTiO_3$/graphene materials were prepared by chemical vapour deposition method (He et al. 2018). The photocatalytic activity was tested by degradation of rhodamine B (RhB) under UV irradiation. Sm-doped $BiFEO_3$ catalyst was formed by sol–gel method (Hu et al. 2017). The effect of dopant amount (1, 3, 5, 7 and 10%) on photodegradation of methyl orange (MO) under visible light was studied. The band gaps were found to be 0.17, 2.15, 2.14, 2.13, 2.12 and 2.06 eV for 0, 1, 3, 5, 7 and 10% doping, respectively. The degradation was highest (86%) when doing was 3% which was 1.5 times than bare $BiFeO_3$. Due to the large recyclability and near-zero carbon emission of hydrogen, it is the biggest potential alternative to carbon-based fossil fuels. Fossil fuels are not sufficient for the demand of energy in future. By volume, hydrogen has low energy content but is high energy content among the common. Many attempts have been made for the generation of hydrogen by using photocatalytic water splitting approach and it is the best ways among renewable sources (Chen et al. 2010). Perovskites are very stable crystalline compounds having highly flexible compositions and used for photocatalytic water splitting (Weidenkaff 2004). Because of redox properties of perovskites, they are used for photocatalytic hydrogen generation. Many photocatalysts such as oxides, mixed oxides, nitrides, sulphides, phosphides have been employed so far for photocatalytic water splitting or H_2 generation from other precursors. However, it is still a challenge to find a material with exceptional activity and can be used without precious metals as co-catalysts. Among various catalysts other than metal oxides, perovskites have been widely utilized and explored for generation (Moniruddin et al. 2018). Perovskites have some advantages over the other catalysts as:

- Suitable band edge potential—for H_2 evolution on cathode and O_2 on anode.
- Flexibility of structure—A or B site for doping.
- Ferroelectric and piezoelectric properties.

Potassium niobate ($KNbO_3$) exhibits unique properties in optic, acoustic, electronic and piezoelectric applications. Carbon-doped $KNBO_3$ photocatalyst was prepared by combination of hydrothermal route and post-calcination. The catalyst possessed excellent photocatalytic activity with high H_2 production under simulated solar light. C-$KNbO_3$ calcined at 350 °C showed highest photocatalytic hydrogen generation (211 μmol g^{-1} h^{-1}) which is 42 times that of bare $KNbO_3$. The catalyst also performs well under visible light illumination (Yu et al. 2018).

$LaTi_2O_7$ is formed by slabs with perovskites like array and separated by La^{3+} layers, and this shows a photonic efficiency of 12% which is used for water dissociation in H_2 and O_2 (Kim et al. 2005). For increasing the photoactivity of this semiconductor, it was doped with BaO so that its efficiency reached up to 50% with the help of a NaOH solution. Table 7 lists some of perovskite-based photocatalysts for various environmental catalysis applications. Oxides with perovskites structure are promising in various applications. Due to their crystalline flexible symmetry, incorporation of different cations leads to formation of materials with different properties. It is thus possible to tune their properties as structure, shape and band gap, which promises a splendid future in photocatalytic applications. Figure 4 represents the

Table 7 Some perovskite-based photocatalysts with their band gap and applications

S. no.	Photocatalysts	Band gap (eV)	Application	References
1.	$SrTiO_3$	3.25	Stoichiometric water splitting	Townsend et al. (2012)
2.	$CaTiO_3$	3.6	For water decomposition	Zhang et al. (2010)
3.	$CoTiO_3$	2.28	Photocatalytic O_2 evolution	Qu et al. (2014)
4.	$NiTiO_3$	2.16	Degradation of nitrobenzene	Qu et al. (2012)
5.	$FeTiO_3$	2.8	Degradation of 2-propenol	Kim et al. (2009)
6.	$AgTaO_3$	3.4	For overall water splitting	Ni et al. (2013)
7.	Sr_2FeNbO_6	2.06	Hydrogen evolution	Borse et al. (2012)
8.	$PrFeO_3$	–	Hydrogen evolution reaction	Tijare et al. (2014)
9.	$PbTiO_3$	2.75	Effective charge separation and photocatalytic performance	Li et al. (2012)
10.	$AgTaO_3$	3.4	Overall water splitting	Ni et al. (2013)
11.	$KNbO_3$	3.14	Water splitting	Wang et al. (2013)
12.	$LaFeO_3$	2.1	Hydrogen evolution	Li et al. (2009a)
13.	$BiFeO_3$	2.3	Visible light photocatalysis	Gao et al. (2007)
14.	$YFeO_3$	2.43	Rh B Degradation	Saeed et al. (2018)

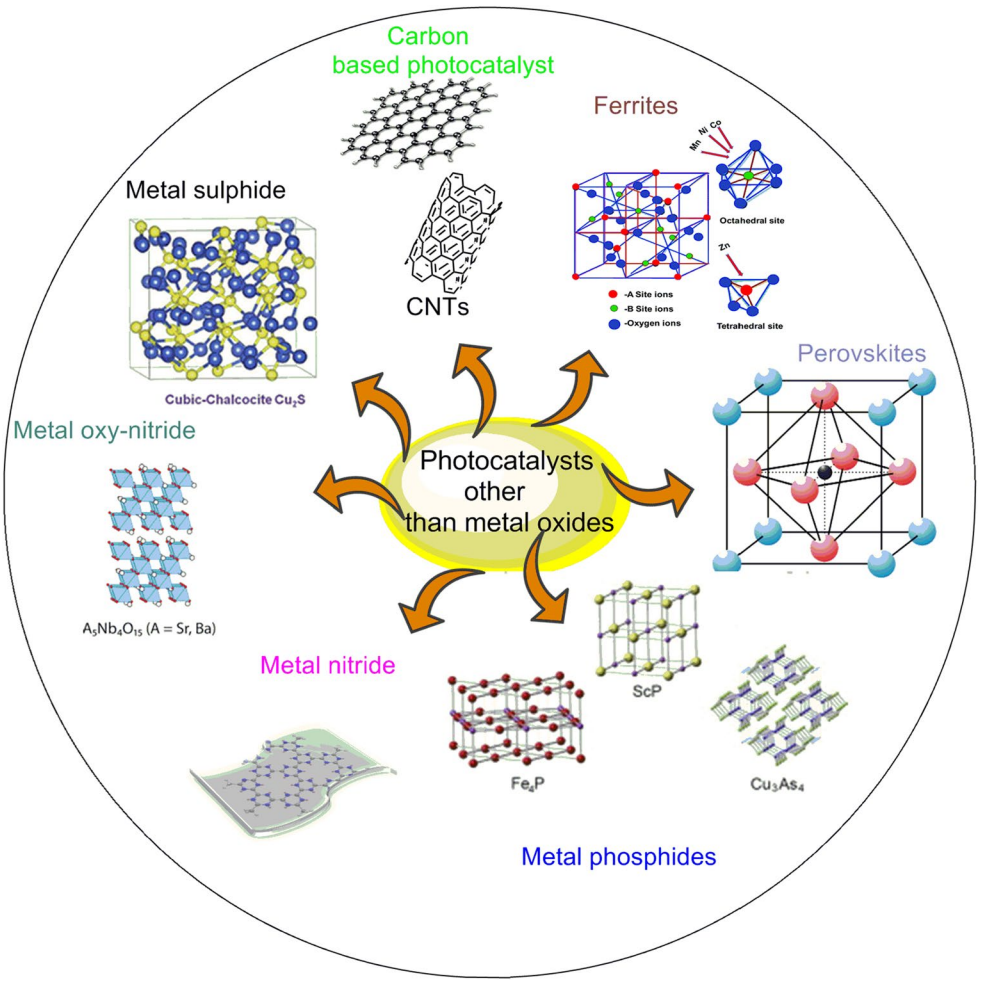

Fig. 4 Various photocatalysts that are used as alternative to metal oxide photocatalysts. CNT: carbon nanotubes

different types of alternative photocatalytic other than metal oxides.

Advantages over metal oxides

Metal oxide-based photocatalysts have a great technological importance in electronics and in environmental remediation. In fact, firstly these oxides were mainly used for each environmental remediation, and among these TiO_2 and ZnO, WO_3 was mainly used. But the upcoming needs and demands of earlier technology and environment pollution and other organic pollutants affecting aquatic lives and human lives lead to search for some other photocatalysts based on metal sulphides, nitrides, ferrites, chalcogenides, oxyhalides and so on as they have good novel photocatalytic activities as compared to metal oxide-based photocatalysts (Kumar et al. 2017b). The good features of photocatalytic system are desirable band gap, high surface area, suitable morphology, stability and reusability (Kumar et al. 2017a; Sharma et al. 2018b). And these above-mentioned photocatalysts have been synthesized and used as alternative to metal oxide-based photocatalysts.

These materials are not particularly derived from metal oxides; they are completely different compounds with different structures and compositions. Mixed oxides of metal like Nb, V or Ta are investigated as alternative photocatalysts. Sulphide- and nitride-based photocatalysts are used for photoactivity in visible range (Kudo and Miseki 2009). Other alternative photocatalysts are:

- Nitride-based photocatalyst, i.e. tantalum nitride having optical properties, fundamental parameters, electronic properties and band gap position, is used for the photocatalytic water redox reaction.
- Perovskite-based photocatalyst is used for the conversion of glucose to H_2 and in visible light photocatalysis.
- Nowadays for the degradation of synthetic dyes, the ferrite-based photocatalyst such as cobalt ferrite, magnesium ferrite, zinc ferrite is used, because these photocatalysts have high photocatalytic activity under visible light.
- Metal sulphide-based photocatalysts such as ZnS, SnS are used for photocatalytic hydrogen production because these sulphides have good solar spectrum response.

New, cheap and hybrid photocatalysts have been achieved, which can be used for contaminate removal, microbial disinfection and energy production. They have proven to be more effective in visible and natural sunlight and have reduced toxicity too. Thus, a shift has been made from conventional photocatalysts to tuneable smart hybrid systems which offer more.

Environmental applications

The major works reported in the field of metal oxide free photocatalysts for environmental detoxification have been studied in the previous sections. This section presents an overview of the type of environmental applications for which these catalysts are being used for a better insight. These include organic and inorganic contaminant removal from water, CO_2 photoreduction, NO_x removal, heavy metal reduction, photokilling of microbes and H_2 production. Figure 5 graphically shows the applications of these alternative photocatalysts in environmental detoxification and clean energy production.

Aqueous pollutants remediation

Increasing exploitation of resources and rising pollution has decreased the water and air quality. Clean water which is a vital prerequisite of life has been polluted with big challenges in developing economies. Various contaminants such as organic, inorganic and microbial have risen to alarming levels posing threat to aquatic and human life. The major toxic effluents in water bodies include dyes, phenols, cosmetics, personal care products, paints, hospital discharges, pharmaceutical wastes, heavy metals and pesticides, which are generally carcinogenic and endocrine disrupting (Kahlon et al. 2018; Sharma et al. 2017e). In addition to dyes and phenols, antibiotics and other drugs have led to high contamination and increase in drug-resistant bacteria which is dangerous for animal and human life. Heterogeneous photocatalysis using semiconductors have been most promising technology for water treatment because it ensures complete mineralization of the contaminants.

Physical approaches like adsorption, flocculation, reverse osmosis are non-destructive, transfer the pollutants to different media and give rise to secondary pollution (Belver et al. 2006). The advanced oxidation process has a potential for pollutant degradation and wastewater

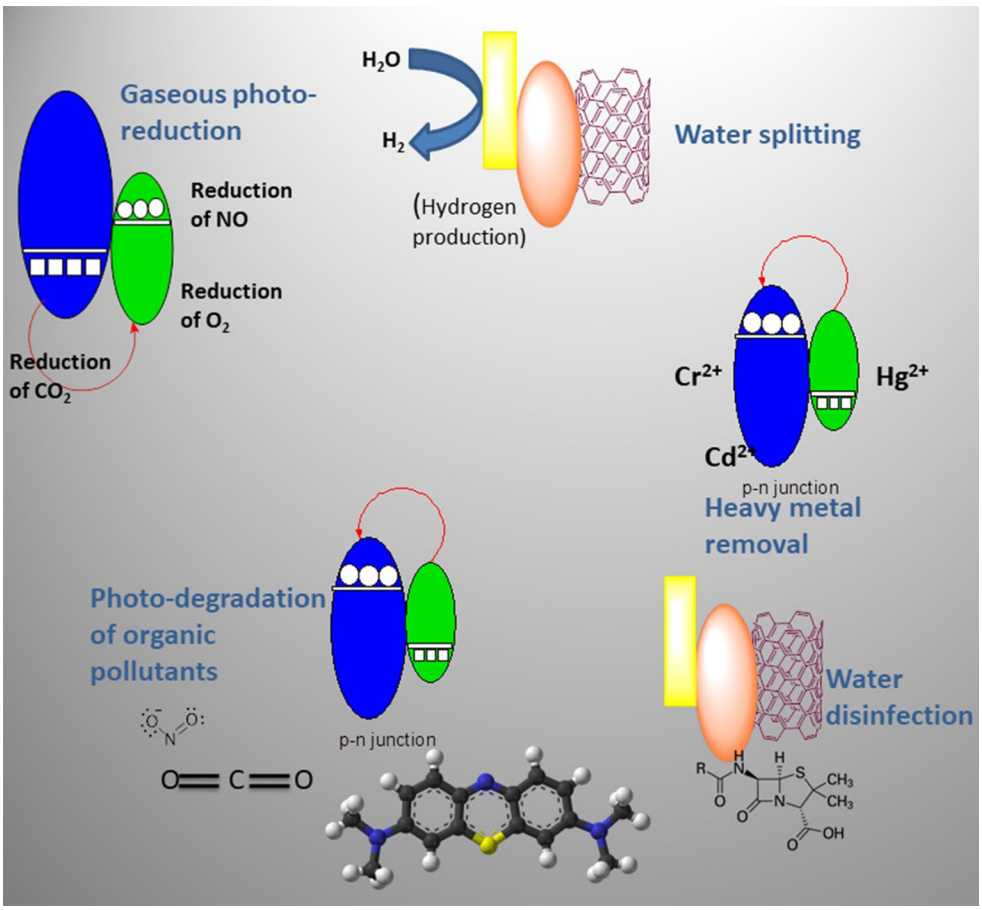

Fig. 5 Environmental applications of alternative photocatalysts. Noteworthy, each class cannot be applied in all these applications with excellent results. Hence, combinations are generally made by researchers for better results or multi-field applications

treatment (Bouzaida et al. 2004). The organic pollutants act as substrate for bacterial growth in natural water mingled with heavy metals such as Fe, Pb, Mn making it harder to remove. Advanced oxidation process has also many applications in this purpose. This process decreases the organic content in water and has advantage that it does not leave any toxic by-products or waste (Kumar et al. 2015; Sharma et al. 2017a). Photocatalysis is a very effective tool to treat organic pollutants in air. This process of photocatalysis may be employed for less humidified indoor environments (Jo and Kim 2009). Many indoor air pollutants such as radiations, formaldehyde and VOC cause various serious health problems. For the removal of air pollution through traffic, the photocatalytically active materials can be added to surface of pavement and building materials (Chen and Poon 2009).

Nowadays researchers are investigating photocatalytic materials other than from metal oxides for water disinfection. There are many organic pollutants such as organic dyes which contaminating the water (Sharma et al. 2017d; Surendhiran et al. 2017). The thermodynamic requirements of the photocatalyst for pollutant degradation are differ from those used in water splitting. For the mineralization of water, the reduction potential of electron in conduction band must be negative, so that it reduces adsorbed molecular oxygen to superoxide. And in valence band their reduction potential must be positive to react with organic matter (Sharma et al. 2017c). Work on water detoxification is mainly focused on other oxide compounds. New research other than TiO_2-based photocatalyst is being done for the water disinfection (Miyauchi et al. 2002). Photocatalysts based on metallate are also used for this purpose under visible light illumination. $BiVO_4$ is the first metallate used for the disinfection of water (Ammar et al. 2006). Tungstate-based photocatalysts are also used for the degradation of aqueous pollutants. The other photocatalysts are $ZnWO_4$, $PbWO_4$, and Bi_2WO_6. But $ZnWO_4$ and $PbWO_4$ have lower activity than Bi_2WO_6 (Ye et al. 2008).

Bi_2WO_6 nanocrystals have various morphologies as nanoflower, nanoplates, knot shape, rod like and were synthesized by hydrothermal method by varying pH, solvents and temperatures. Photocatalytic activity of the photocatalysts was evaluated by degradation of ceftriaxone sodium under visible light irradiation (Zhao et al. 2018b). In another work, silver/silver chloride/exfoliated graphite (Ag/AgCl/EG) photocatalyst was prepared by precipitation and photoreduction route. The catalyst exhibited efficient visible light photocatalytic activity with 99.5% rhodamine B and 89.1% phenol removal (Gou et al. 2018). In a modification of g-C_3N_4, a *p–n*-type Bi_5O_7I/g-C_3N_4 nanoheterojunction was prepared by template and annealing-hydrothermal co-deposition method (Dong et al. 2018). The photocatalytic activity of Bi_5O_7I/g-C_3N_4 is about 30 times that of the unmodified sample.

CO_2 reduction, NO_x removal and heavy metal reduction

The increasing levels of CO_2 in atmosphere due to industrial pollution and extensive use of fuels have aroused a great concern because of global warming. The exhaustive exploitation of fuels has led to energy crisis and demand for novel ideas for clean energy production. The photocatalytic reduction of CO_2 into CO, CH_4, CH_3OH, etc. has been the most effective and inexpensive route. In a typical reaction, the holes from valence band generate protons ($E^\circ = 0.82$ eV vs. NHE). Secondly, CO_2 is reduced by electrons from conduction band ($E^\circ = -0.24$ eV).

Photocatalysts with zeolites and mesoporous material are also used for treating gaseous contamination. As the properties of zeolites are not good for photocatalytic activity, some remarkable results are obtained in gas phase treatment. Artificial photosynthesis of hydrocarbons from CO_2 and water is also a good matter of research. There are many problems rising because of the increase in concentration of CO_2 in atmosphere. Many references tell that the CO_2 photoreduction is only possible with TiO_2-based photocatalysts, but it is not only the material for this purpose. From the carbon dioxide reduction process, methanol is the valuable product because it is directly used an alternative fuel by chemical industry. Higher yield is required over NiO and ZnO then over to TiO_2 for the photoalteration of carbon dioxide into methanol in aqueous phase (Yahaya et al. 2004). In the photoreduction of carbon dioxide, the Ti-incorporated mesoporous silica has more activity than bulk TiO_2 and generated methanol and methane under UV irradiation (Hwang et al. 2005; Su et al. 2016). However, it cannot be considered as a pure photocatalytic process. For the CO_2 photoreduction process, methanol is the most valuable product because it can be used as an alternative fuel or building block by the industry. Higher yields were obtained over NiO and ZnO than over TiO_2 for the photoconversion of CO_2 into methanol in aqueous phase (Yahaya et al. 2004). Highly photoactive and stable photocatalysts 2D/2D zinc vanadium oxide-reduced Graphene Oxide ZnV_2O_6/RGO were synthesized by hydrothermal method (Bafaqeer et al. 2018).

The catalysts were used for photoreduction of CO_2 into CH_3OH, CH_3COOH and HCOOH under visible light. The yield of CH_3OH is 3254 μmol g^{-1}, which was 5.5 times than that of ZnO/V_2O_5. The selectivity of catalyst for CH_3OH is 68.89%, which is quite high as compared to popular metal oxides. Metal-based semiconductors have been used extensively for CO_2 reduction. Non-metal-based and metal-free semiconductors have activity comparable to metal-based photocatalysts. Among all metal-free semiconductors, g-C_3N_4 is the most promising one. In a related work, Cu-modified g-C_3N_4 (Cu/g-C_3N_4) as photocatalysts was synthesized for simulated solar energy powered conversion of CO_2 into CH_4 and CH_3OH. The yield of CH_4 by 3% Cu/g-C_3N_4

was 109 mol g^{-1} h^{-1}, which was significantly higher than pure g-C_3N_4 (Tahir et al. 2017). In another modification to g-C_3N_4, $LaPO_4$/g-C_3N_4 core–shell nanowires via hydrothermal technique and used for photocatalytic CO_2 reduction. The coating leads to high absorption and higher charge transfer. A maximum CO amount of 0.433 mol was produced in 1 h using 30 mg photocatalyst (Li et al. 2017a). Metal nitrides are also promising catalysts for CO_2 conversion into fuels without any noble metal as co-catalyst. In bismuth-modified Ta_3N_5 (Ta_3N_5/Bi), the doping leads to higher CH_4 production which is 5 times more than bare Ta_3N_5 (Wang et al. 2018a). Pollutants such as NO_X are apparently removed from environment as they are causing harm to living things in the world. These inorganic compounds like (NO_x, NO, etc.) present at ppm concentration in air. The photocatalytic treatment of air centres on the mineralization of organic compounds (Demeestere et al. 2007) receives less attention as compared to other applications of alternative photocatalyst. Mixed oxynitrides, oxyhalides and carbide-based photocatalysts are used for the removal of gaseous contaminants. $SrTiO_3$ is an interesting photocatalysts, but it is only activated in UV region because it has high band gap (Chen et al. 2009). For the destruction of NO, the $SrTiO_3$ has been doped with N, F or La. As compared to TiO_2, the photocatalytic performance of this material was 1.4 times greater.

The semiconductor photocatalysis is also used for abatement of other toxic gases as nitrogen oxides (NO_x). The air pollution due to NO_x, i.e. NO and NO_2 has increased alarmingly due to extensive combustion of fuels and industrial pollution. The minimum levels of NO_x as set by national and international regulating agencies have surpassed in major cities of the world. NO_x is the major cause of acid rains and photochemical smog, which are an environmental and human health concern. Removal of NO is necessary as it is major source for other NO_x gases. Conventional methods to remove NO include catalytic decomposition, reduction and wet scrubbing. However, these methods are applicable where the concentration of NO is high. But for lower levels as parts per billion (ppb), these techniques become less effective and costly too. Photocatalytic decomposition of NO is an emerging and promising field. During a semiconductor photocatalytic reaction, the hydroxyl and superoxide radicals produce NO_2 and NO_3^- which may also be toxic. Thus, the presence of hydrogen in reaction mixture leads to the formation of N_2 and NH_3. This solves the problem of release of highly toxic gases and synthesis of NH_3 by photocatalytic process. The two-dimensional BiOCl/$Bi_{12}O_{17}Cl_2$ nanojunction was fabricated by in situ method and was used for removal of NO at ppb level (Zhang et al. 2018c). The optical band gaps of BiOCl, $Bi_1O_{17}Cl_2$ and BiOCl/$Bi_{12}O_{17}Cl_2$ were found to be 3.20, 2.43 and 2.77 eV, respectively. 37.2% of NO was removed in the presence of the nanojunction.

$SrTiO_3$ catalyst decorated with $SrCO_3$ was prepared by one-step in situ pyrolysis and was used for the photocatalytic removal of NO. $SrCO_3$ not only increased the NO removal but also helped in keeping $SrTIO_3$ activated during the process. Forty-seven percentage removal efficiency in 12 min was achieved (Jin et al. 2018). This enhanced activity due to the formation of a junction is similar to the surface-deposited noble metals. N-doped $Bi_2O_2CO_3$/graphene oxide composite was synthesized by one-pot hydrothermal route. The catalysts were used to degrade NO_x in visible light with the sample containing 1% GO showing the highest activity. As compared to pure GO, the N-doping improves the photocatalytic degradation of NO. This leads to 74.6% NO removal and complete inhibition of NO_2 generation. The high activity is ascribed to extended absorption and high separation of charge carriers (Chen et al. 2018).

Among other contaminants, heavy metal ions which are generally present in waste water and air have acute toxicity and dangerous for ecosystem (Sharma et al. 2016b). Cr(VI) is a major contaminant these days because of its carcinogenic and teratogenic nature (Kumar et al. 2016). It has been regarded as one of the priority pollutants. On the other hand, Cr(III) is an essential trace element. One of the strategies for removal of Cr(VI) is adsorption; however, it just transfers the medium and potential danger still remains in the system. Other methods include chemical reduction and electrodeposition, but these are complex and expensive. Photocatalytic reduction of Cr(VI) into Cr(III) is an preferred method because it is fast, effective and cheap. In particular, reduction in the presence of natural sunlight is an attractive technology. The electrons generated on photoexposure lead to the formation of Cr(III) and are effective in acidic medium.

Among metal-free semiconductors, g-C_3N_4 is an promising candidate for the Cr(VI) reduction. The conduction band of g-C_3N_4 is usually more negative than that required for Cr(VI)/Cr(III), i.e. − 1.3 eV (vs. NHE). Hence, thermodynamically it can easily reduce. However, the band edge can be shifted to more negative by suitable structural modification or by doping.

Sulphur-doped g-C_3N_4 microspheres were prepared from condensation of trithiocyanuric acid. The photocatalytic activity was tested for reduction of Cr(VI) in visible light in neutral aqueous solution. 90% Cr(VI) was reduced in 3 h using sample with 1% sulphur doping (Cui et al. 2018b). Ren et al. (2017) prepared carbon quantum dots (CQDs) decorated with $MoSe_2$ photocatalysts for photocatalytic reduction of Cr(VI). 99% reduction was reported when the amount of CQDs was 1%. The increase in the activity was attributed to enhanced optical absorption, high charge transfer and light down-converting effect from CQDs. For increasing the efficiency and the reaction time, heterostructures or composite catalysts are involved. In a related work, $ZnFe_2O_4$/CdS composites were prepared by a facile route (Fang et al. 2018).

7% $ZnFe_2O_4$/CdS can effectively reduce more than 90% Cr(VI) in 120 min, which is faster than the single catalysts. In another work, metal-free catalyst boron nitride (BN) was coupled with BiOCl flower-shaped microspheres (Xu et al. 2017). 1% BN/BiOCl exhibited highest activity which is about 2.39 times than that of pure BiOCl. However, for 2% BN/BiOCl the activity decreased because of BN occupying some of active sites of BiOCl. Many other heterojunctions and composite materials have been reported in the literature for photoreduction of Cr(VI) for better performance, and research is still going for achieving the best.

Water splitting and clean energy production

The clean energy production is essential because of the increasing depletion of fossil fuels. In this regard, hydrogen is one of the most prospective energy sources. The hydrogen is generally produced by electrocatalytic and photocatalytic water splitting as well as from other sources too. In general, precious metals such as Pt, Ir and Pd are used as co-catalysts in hydrogen production and have excellent performance. But they are scarce and expensive. Therefore, new catalysts which can either be used in combination with these precious metals or which can directly be used without co-catalyst are required. Many reported works have utilized metal oxides and mixed metal oxides for the purpose of the same but with poor efficiency. Photocatalytic generation of H_2 via water splitting is the most efficient and cost-effective methodology.

For applying this process to energy storage, the temperature of 2500 K is required. To degenerate the water molecule, photochemical decomposition of water is a good alternative because photon has a shorter wavelength than 1100 nm. The photocatalytic splitting of pure water is done under visible light and ultraviolet light. Various techniques are used for the conversion of solar energy into electricity or chemical energy but photovoltaic being the most direct. For this, photoelectrochemical process is mostly used (Sfaelou and Lianos 2016). Photoactivated fuel cells also named as photocatalytic fuel cell or photofuel cells are used to oxidize a fuel which produces electricity or storable chemical energy mainly by hydrogen. Photoelectrochemical cell has a photoanode electrode which carries photocatalyst. For the water splitting purposes, perovskite-based photocatalysts are also used. In water splitting reaction, the photon of suitable wavelength, electrons and holes is produced within photocatalyst. Water molecules are absorbed on the surface of photocatalyst because of interaction of water molecule and hole in the valence band.

As the most promising way to generate hydrogen as a clean and renewable fuel, the evolution of hydrogen and oxygen using sunlight is considered (Tang et al. 2008). For the water treatment technology, heterogeneous photocatalysis is the most effective technique. It has high efficiency in the degradation of organic contaminants and disinfection of pathogenic microorganism (Chong et al. 2010). The photocatalytic water splitting of pure water under UV light is also done with the help of perovskites titanates such as $SrTiO_3$. This shows reduced activity for the cleavage of water molecule (Domen et al. 1980). Among perovskites, lanthanum titanate $La_2Ti_2O_7$ shows a photonic efficiency of 120% for water dissociation in O_2 and H_2 (Kim et al. 2005). Many nitrides, mixed chalcogenides and perovskites have been successfully used with and without co-catalysts for H_2 production.

Hybrid photocatalysts

However, many new photocatalysts have been employed as alternative to metal oxides with better properties. But combination of various catalysts is required for faster and better results. These hybrid materials which involve combination of semiconductors with other catalysts, polymers, biomolecules, sensitizers, organic frameworks, supports, have high photoactivity, adsorption potential and highly reduced recombination of charge carriers. These hybrid materials may contain photoactive metal oxides (Colmenares and Xu 2016; Zhao et al. 2016b), quantum dots or perovskites (Wang et al. 2015b) enhancing the photocatalytic efficiency. For the photocatalytic supports, there are various types of synthetic polymer like polythene, polypropylene, polystyrene, poly vinyl chloride and so on (Colmenares and Kuna 2017). In order to know the restrictions of photocatalytic achievements, the main photochemical and photophysical mechanism leading to that process must be known. In this regard, semiconductor heterojunction or assemblies which involve two or more semiconductors combined at nanoscale with a high interfacial contact have proved to be an effective strategy. The coupling of semiconductors is done after considering the band gaps, position of conduction band and valence band edges. This can be done to promote effective movement and separation of photogenerated electrons and holes. The *p*-type (like BiOCl, Cu_2O, etc.) and n-type semiconductors are combined to form heterojunctions. And there is a diffusion of electrons and holes even in the absence of the light, which generated an intrinsic electric field. This field facilitates the movement of electrons among conduction bands and that of holes between the valence bands. In addition, many researchers utilize electron sinks as polymers, carbon, biochar, graphene oxide and reduced graphene oxide into the catalyst for eating up unused electrons which decreases recombination.

Table 8 lists some of the hybrid photocatalysts which are not based on metal oxides and employ sulphides, nitrides, oxyhalides, halides, graphitic materials and perovskites as the candidates. It is certain that they perform better in

Table 8 Some hybrid photocatalysts for environmental applications

S. no.	Photocatalyst	Photocatalytic performance	References
1.	CuS/C_3N_4	Complete MB elimination in 90 min	Khan et al. (2018)
2.	Ag_2WO_4/g-C_3N_4 nanosheets	Complete RhB and MO removal in 20 min	Li et al. (2016b)
3.	ZnS@CdS–Te	H_2 production (~600 µmol h^{-1})	Xin et al. (2018)
4.	Rh-loaded $CsTaWO_6$	H_2 production (~8 µmol h^{-1})	Weller et al. (2017)
5.	SiC/C_3N_4	RhB removal/~70% in 150 min	Chang et al. (2018)
6.	Rh-loaded $AgGaS_2$	H_2 production (944 µmol h^{-1})	Kudo (2006)
7.	$La_2Ti_2O_7$	H_2 production (72.46 µmol h^{-1})	Song et al. (2007)
8.	Ni_2P-/Fe-doped g-C_3N_4	H_2 evolution (397 µmol h^{-1} g^{-1})	Liu et al. (2017a)
9.	CdS nanoflowers	H_2 evolution rate of 5.98 mmol h^{-1}	Liu et al. (2018)
10.	ZnS@CdS–Te	H_2 evolution rate of 600 mmol h^{-1}	Xin et al. (2018)
11.	$Ni_2P/CaIn_2S_4$	H_2 evolution rate of 486 µmol h^{-1} g^{-1}	Wang et al. (2018b)
12.	Ba:$La_2Ti_2O_7/NiO_X$	H_2 evolution rate of 474 µmol h^{-1}	Kim et al. (2005)
13.	Pt/K@C_3N_4	H_2 evolution rate of 1337.2 µmol h^{-1}	Wang et al. (2018c)
14.	CdS-diethylenetriamine	H_2 evolution rate of 8095.5 µmol h^{-1} g^{-1}	Lv et al. (2018)
15.	Ag–AgCl–$CaTiO_3$	H_2 evolution rate of 226.53 µmol h^{-1} g^{-1}	Jiang et al. (2018)
16.	CdS/Fe_2P	H_2 evolution rate of 220 µmol h^{-1} g^{-1}	Pan et al. (2018)
17.	Ag–$NiTiO_3$:V	95% RhB removal in 120 min	Mi et al. (2018)
18.	CdS/MoS_2	H_2 evolution rate of 1032.1 µmol h^{-1}	Sun et al. (2018)
19.	Pd–$GdCrO_4$	100% nitrate reduction in 100 min	Hou et al. (2018)
20.	Ag–SiC	68% removal of Orange G and 96% Amido Black 10B 240 min under UV light	Adhikari et al. (2018)
21.	$BiVO_4$/N-RGO	Photodegradation of metronidazole (MTZ) and chloramphenicol (CAP)/95% MTZ and 93% CAP removal in 90 min	Appavu et al. (2018)
22.	2D/2D ZnV_2O_6/RGO	Photoreduction of CO_2 into CH_3OH, CH_3COOH and HCOOH/conversion to main product CH_3OH—5154 µmol g^{-1} cat^{-1}	Bafaqeer et al. (2018)
23.	AgCl@Ag@TiO_2	Inactivation of *Escherichia coli* K12. (77% inactivation)	Tian et al. (2014)
24.	CdS/BiOBr	MG degradation (99% removal in 1.5 h)	Cui et al. (2018a)
25.	$CuInS_2$/ZnS/TGA	RhB degradation (~60% in 1 h)	Zhang et al. (2017c)
26.	Acidified g-C3N4/g-C3N4	MO degradation (96. % in 150 min)	Yang et al. (2016)
27.	Pd/$GdCrO_3$	Photocatalytic reduction of nitrate into N_2 (98.4%)	Hou et al. (2018)
28.	BiOBr/$FeWO_4$	Degradation of doxycycline (90% in 1 h)	Gao et al. (2018)
29.	$BiPO_4/Bi_2S_3$	Degradation of MB (100% removal)	Lu et al. (2015)
30.	$BaNb_{0.5}Ta_{0.5}O_2N$	Photocatalytic water oxidation (150.7 µmol O_2 evolved in 5 h)	Kawashima et al. (2017)
31.	Graphene oxide/$AgIO_4$	79.4% MO, 96.8% and 90.8% MB removal in 40 min	Ji et al. (2017)
32.	g-C_3N_4/GO aerogel	MB, MO (~90% in 40 min), bromate reduction (80% in 60 min)	Tang et al. (2017)

These include polymer composites, heterojunctions, layered compounds and nanoassemblies

all photocatalytic applications as compared to the single catalysts.

Conclusion

Metal oxides have ruled the advanced oxidation processes for environmental detoxification and have been star photocatalysts so far. But with changing scenario, the energy demands for increasing and more emerging pollutants of concern are increasing. In addition, the efficiency, quantum yield, reusability, toxicity and cost-effectiveness of the photocatalyst decide its role in real conditions, outside the laboratory. There have been innovations reported for improvement of activity of metal oxides. However, as discussed they also possess many limitations. As it has been stated in this review, a number of alternative photocatalysts have surpassed the performance of metal oxides for various environmental applications under different experimental constrains. These photocatalysts mainly include mainly sulphides, nitrides, halides, oxyhalides, perovskites, metal-free materials and hybrid catalysts which posses better photocatalytic activity along with the better use of the solar spectrum.

Many photocatalysts such as some nitrides and perovskites have been used for photocatalytic water splitting and

CO_2 conversion without the help of any precious metals as co-catalysts or support. However, this was not achieved earlier with popular metal oxides. Involving representative elements and non-metals into photocatalysis has remained a challenge; however, nitrides, phosphides, carbides, sulphides, BN, g-C_3N_4, etc. have scaled down the cost of photocatalysis as well as increased the bio-quotient of the catalyst because of low toxicity. The designing of an optimum photocatalyst with a simple approach for solar utilization, high quantum efficiency, reusability, separation and low toxicity has been a synthetic challenge. In addition to increasing environmental pollution and exploitation of non-renewable energy sources, the next challenge is to develop novel materials and novel green technologies with a multi-pronged approach. It has been observed that many of photocatalytic experiments performed in the laboratories for detoxification and energy production have not been able to materialize in the real world. Thus, it is necessary to develop sustainable systems which utilize the advanced oxidation processes to detoxify environment and produce clean energy in the real and practical situations.

References

Adeli B, Taghipour F (2016) Facile synthesis of highly efficient nanostructured gallium zinc oxynitride solid solution photocatalyst for visible-light overall water splitting. Appl Catal A 521:250–258. https://doi.org/10.1016/j.apcata.2016.01.001

Adhikari S, Eswar NK, Sangita S, Sarkar D, Madras G (2018) Investigation of nano Ag-decorated SiC particles for photoelectrocatalytic dye degradation and bacterial inactivation. J Photochem Photobiol A 357:118–131. https://doi.org/10.1016/j.jphotochem.2018.02.017

Ammar S, Abdelhedi R, Flox C, Arias C, Brillas E (2006) Electrochemical degradation of the dye indigo carmine at boron-doped diamond anode for wastewaters remediation. Environ Chem Lett 4:229–233. https://doi.org/10.1007/s10311-006-0053-2

An X et al (2017) Graphitic carbon/carbon nitride hybrid as metal-free photocatalyst for enhancing hydrogen evolution. Appl Catal A 546:30–35. https://doi.org/10.1016/j.apcata.2017.07.046

Anchieta CG et al (2014) Effects of solvent diols on the synthesis of $ZnFe_2O_4$ particles and their use as heterogeneous photo-Fenton catalysts. Materials 7:6281–6290. https://doi.org/10.3390/ma7096281

Anpo M, Kim T-H, Matsuoka M (2009) The design of Ti-, V-, Cr-oxide single-site catalysts within zeolite frameworks and their photocatalytic reactivity for the decomposition of undesirable molecules—the role of their excited states and reaction mechanisms. Catal Today 142:114–124. https://doi.org/10.1016/j.cattod.2008.11.006

Ansari SA, Khan MM, Kalathil S, Nisar A, Lee J, Cho MH (2013) Oxygen vacancy induced band gap narrowing of ZnO nanostructures by an electrochemically active biofilm. Nanoscale 5:9238–9246. https://doi.org/10.1039/C3NR02678G

Appavu B, Thiripuranthagan S, Ranganathan S, Erusappan E, Kannan K (2018) $BiVO_4$/N-rGO nano composites as highly efficient visible active photocatalyst for the degradation of dyes and antibiotics in eco system. Ecotoxicol Environ Saf 151:118–126. https://doi.org/10.1016/j.ecoenv.2018.01.008

Arai T, Senda SI, Sato Y, Takahashi H, Shinoda K, Jeyadevan B, Tohji K (2008) Cu-doped ZnS hollow particle with high activity for hydrogen generation from alkaline sulfide solution under visible light. Chem Mater 20:1997–2000. https://doi.org/10.1021/cm071803p

Attia EF, Zaki AH, El-Dek SI, Farghali AA (2017) Synthesis, physicochemical properties and photocatalytic activity of nanosized Mg doped Mn ferrite. J Mol Liq 231:589–596. https://doi.org/10.1016/j.molliq.2017.01.108

Bafaqeer A, Tahir M, Amin NAS (2018) Synergistic effects of 2D/2D ZnV_2O_6/RGO nanosheets heterojunction for stable and high performance photo-induced CO_2 reduction to solar fuels. Chem Eng J 334:2142–2153. https://doi.org/10.1016/j.cej.2017.11.111

Baran T, Wojtyła S, Dibenedetto A, Aresta M, Macyk W (2015) Zinc sulfide functionalized with ruthenium nanoparticles for photocatalytic reduction of CO_2. Appl Catal B 178:170–176. https://doi.org/10.1016/j.apcatb.2014.09.052

Batista AP, Carvalho HWP, Luz GH, Martins PF, Gonçalves M, Oliveira LC (2010) Preparation of CuO/SiO_2 and photocatalytic activity by degradation of methylene blue. Environ Chem Lett 8:63–67. https://doi.org/10.1007/s10311-008-0192-8

Belver C, Bellod R, Fuerte A, Fernández-García M (2006) Nitrogen-containing TiO_2 photocatalysts. Part 1. Synthesis and solid characterization. Appl Catal B Environ 65:301–308. https://doi.org/10.1016/j.apcatb.2006.02.007

Borse P et al (2012) Improved photolysis of water from ti incorporated double perovskite Sr_2 $FeNbO_6$ lattice. Bull Korean Chem Soc 33:3407–3412. https://doi.org/10.5012/bkcs.2012.33.10.3407

Bouzaida I, Ferronato C, Chovelon JM, Rammah ME, Herrmann JM (2004) Heterogeneous photocatalytic degradation of the anthraquinonic dye, Acid Blue 25 (AB25): a kinetic approach. J Photochem Photobiol A 168:23–30. https://doi.org/10.1016/j.jphotochem.2004.05.008

Burton LA et al (2013) Synthesis, characterization, and electronic structure of single-crystal SnS, Sn_2S_3, and SnS_2. Chem Mater 25:4908–4916. https://doi.org/10.1021/cm403046m

Buscema M, Groenendijk DJ, Blanter SI, Steele GA, van der Zant HSJ, Castellanos-Gomez A (2014) Fast and broadband photoresponse of few-layer black phosphorus field-effect transistors. Nano Lett 14:3347–3352. https://doi.org/10.1021/nl5008085

Cai Y et al (2018) Synthesis of BiOCl nanosheets with oxygen vacancies for the improved photocatalytic properties. Appl Surf Sci 439:697–704. https://doi.org/10.1016/j.apsusc.2018.01.089

Callejas JF et al (2014) Electrocatalytic and photocatalytic hydrogen production from acidic and neutral-pH aqueous solutions using iron phosphide nanoparticles. ACS Nano 8:11101–11107. https://doi.org/10.1021/nn5048553

Cao QW, Zheng YF, Yin HY, Song XC (2016) A novel AgI/$AgIO_3$ heterojunction with enhanced photocatalytic activity for organic dye removal. J Mater Sci 51:4559–4565. https://doi.org/10.1007/s10853-016-9769-y

Carp O, Huisman CL, Reller A (2004) Photoinduced reactivity of titanium dioxide. Prog Solid State Chem 32:33–177. https://doi.org/10.1016/j.progsolidstchem.2004.08.001

Chang F, Zheng J, Wang X, Xu Q, Deng B, Hu X, Liu X (2018) Heterojuncted non-metal binary composites silicon carbide/g-C_3N_4 with enhanced photocatalytic performance. Mater Sci Semicond Process 75:183–192. https://doi.org/10.1016/j.mssp.2017.11.043

Chen J, Poon C (2009) Photocatalytic construction and building materials: from fundamentals to applications. Build Environ 44:1899–1906. https://doi.org/10.1016/j.buildenv.2009.01.002

Chen L, Zhang S, Wang L, Xue D, Yin S (2009) Preparation and photocatalytic properties of strontium titanate powders via sol–gel process. J Cryst Growth 311:746–748. https://doi.org/10.1016/j.jcrysgro.2008.09.185

Chen X, Shen S, Guo L, Mao SS (2010) Semiconductor-based photocatalytic hydrogen generation. Chem Rev 110:6503–6570. https://doi.org/10.1021/cr1001645

Chen H, Yao J, Qiu P, Xu C, Jiang F, Wang X (2017) Facile surfactant assistant synthesis of porous oxygen-doped graphitic carbon nitride nanosheets with enhanced visible light photocatalytic activity. Mater Res Bull 91:42–48. https://doi.org/10.1016/j.materresbull.2017.02.042

Chen M, Huang Y, Yao J, Cao J-J, Liu Y (2018) Visible-light-driven N-$(BiO)_2CO_3$/Graphene oxide composites with improved photocatalytic activity and selectivity for NO_x removal. Appl Surf Sci 430:137–144. https://doi.org/10.1016/j.apsusc.2017.06.056

Cheng J, Wang Y, Xing Y, Shahid M, Pan W (2017) Surface defects decorated zinc doped gallium oxynitride nanowires with high photocatalytic activity. Appl Catal B 209:53–61. https://doi.org/10.1016/j.apcatb.2017.03.004

Chong MN, Jin B, Chow CWK, Saint C (2010) Recent developments in photocatalytic water treatment technology: a review. Water Res 44:2997–3027. https://doi.org/10.1016/j.watres.2010.02.039

Chowdhury FA, Mi Z, Kibria MG, Trudeau ML (2015) Group III-nitride nanowire structures for photocatalytic hydrogen evolution under visible light irradiation. APL Mater 3:104408. https://doi.org/10.1063/1.4923258

Clark PA, Oyama ST (2003) Alumina-supported molybdenum phosphide hydroprocessing catalysts. J Catal 218:78–87. https://doi.org/10.1016/S0021-9517(03)00086-1

Colmenares JC, Kuna E (2017) Photoactive hybrid catalysts based on natural and synthetic polymers: a comparative overview. Molecules 22:790. https://doi.org/10.3390/molecules22050790

Colmenares JC, Xu Y-J (2016) Heterogeneous photocatalysis. Green Chem Sustain Technol. https://doi.org/10.1007/978-3-662-48719-8

Cui H, Zhou Y, Mei J, Li Z, Xu S, Yao C (2018a) Synthesis of CdS/BiOBr nanosheets composites with efficient visible-light photocatalytic activity. J Phys Chem Solids 112:80–87. https://doi.org/10.1016/j.jpcs.2017.09.011

Cui Y, Li M, Wang H, Yang C, Meng S, Chen F (2018b) In-situ synthesis of sulfur doped carbon nitride microsphere for outstanding visible light photocatalytic Cr(VI) reduction. Sep Purif Technol 199:251–259. https://doi.org/10.1016/j.seppur.2018.01.037

Demeestere K, Dewulf J, Van Langenhove H (2007) Heterogeneous photocatalysis as an advanced oxidation process for the abatement of chlorinated, monocyclic aromatic and sulfurous volatile organic compounds in air: state of the art. Crit Rev Environ Sci Technol 37:489–538. https://doi.org/10.1080/10643380600966467

Dhiman P, Chand J, Kumar A, Kotnala RK, Batoo KM, Singh M (2013) Synthesis and characterization of novel Fe@ZnO nanosystem. J Alloys Compd 578:235–241. https://doi.org/10.1016/j.jallcom.2013.05.015

Dhiman P et al (2017) Nano $Fe_xZn_{1-x}O$ as a tuneable and efficient photocatalyst for solar powered degradation of bisphenol A from aqueous environment. J Clean Prod 165:1542–1556. https://doi.org/10.1016/j.jclepro.2017.07.245

Dillip GR, Sreekanth TVM, Joo SW (2017) Tailoring the bandgap of N-rich graphitic carbon nitride for enhanced photocatalytic activity. Ceram Int 43:6437–6445. https://doi.org/10.1016/j.ceramint.2017.02.057

Ding N et al (2018) Enhanced photocatalytic activity of mesoporous carbon/C_3N_4 composite photocatalysts. J Colloid Interface Sci 512:474–479. https://doi.org/10.1016/j.jcis.2017.10.081

Domen K, Naito S, Soma M, Onishi T, Tamaru K (1980) Photocatalytic decomposition of water vapour on an NiO–$SrTiO_3$ catalyst. J Chem Soc Chem Commun. https://doi.org/10.1039/C3980000054 3

Dong L, Shi C, Guo L, Yang T, Sun Y, Cui X (2017a) Fabrication of redox and pH dual-responsive magnetic graphene oxide microcapsules via sonochemical method. Ultrason Sonochem 36:437–445. https://doi.org/10.1016/j.ultsonch.2016.12.027

Dong Y, Kong L, Wang G, Jiang P, Zhao N, Zhang H (2017b) Photochemical synthesis of Co_xP as cocatalyst for boosting photocatalytic H_2 production via spatial charge separation. Appl Catal B 211:245–251. https://doi.org/10.1016/j.apcatb.2017.03.076

Dong Z et al (2018) The *p*–*n*-type Bi_5O_7I-modified porous C_3N_4 nano-heterojunction for enhanced visible light photocatalysis. J Alloys Compd 747:788–795. https://doi.org/10.1016/j.jallcom.2018.03.112

Du Y, Zhao L, Su Y (2011) Tantalum (oxy)nitrides: preparation, characterisation and enhancement of photo-Fenton-like degradation of atrazine under visible light. J Hazard Mater 195:291–297. https://doi.org/10.1016/j.jhazmat.2011.08.042

Du X, Yao S, Jin X, Long Y, Liang B, Li W (2015) Photocatalytic properties of aluminum oxynitride (AlON). Mater Lett 161:72–74. https://doi.org/10.1016/j.matlet.2015.08.069

Dükkancı M (2018) Sono-photo-Fenton oxidation of bisphenol-A over a $LaFeO_3$ perovskite catalyst. Ultrason Sonochem 40:110–116. https://doi.org/10.1016/j.ultsonch.2017.04.040

Ebbinghaus SG, Abicht H-P, Dronskowski R, Müller T, Reller A, Weidenkaff A (2009) Perovskite-related oxynitrides—recent developments in synthesis, characterisation and investigations of physical properties. Prog Solid State Chem 37:173–205. https://doi.org/10.1016/j.progsolidstchem.2009.11.003

Fang C, Orhan E, De Wijs G, Hintzen H, De Groot R, Marchand R, Saillard J-Y (2001) The electronic structure of tantalum (oxy) nitrides TaON and Ta_3N_5. J Mater Chem 11:1248–1252. https://doi.org/10.1039/B005751G

Fang Z, Zhang L, Yang T, Su L, Chou K-C, Hou X (2017) Cadmium sulfide with tunable morphologies: preparation and visible-light driven photocatalytic performance. Physica E 93:116–123. https://doi.org/10.1016/j.physe.2017.06.003

Fang S, Zhou Y, Zhou M, Li Z, Xu S, Yao C (2018) Facile synthesis of novel $ZnFe_2O_4$/CdS nanorods composites and its efficient photocatalytic reduction of Cr(VI) under visible-light irradiation. J Ind Eng Chem 58:64–73. https://doi.org/10.1016/j.jiec.2017.09.008

Fujishima A, Honda K (1972) Electrochemical photolysis of water at a semiconductor electrode. Nature 238:37. https://doi.org/10.1038/238037a0

Fujishima A, Rao T, Tryk D (2000) Titanium dioxide photocatalysis. J Photochem Photobiol C Photochem Rev 1:1. https://doi.org/10.1016/S1389-5567(00)00002-2

Gao F et al (2007) Visible-light photocatalytic properties of weak magnetic $BiFeO_3$ nanoparticles. Adv Mater 19:2889–2892. https://doi.org/10.1002/adma.200602377

Gao J, Gao Y, Sui Z, Dong Z, Wang S, Zou D (2018) Hydrothermal synthesis of BiOBr/$FeWO_4$ composite photocatalysts and their photocatalytic degradation of doxycycline. J Alloys Compd 732:43–51. https://doi.org/10.1016/j.jallcom.2017.10.092

Goharshadi EK, Hadadian M, Karimi M, Azizi-Toupkanloo H (2013) Photocatalytic degradation of reactive black 5 azo dye by zinc sulfide quantum dots prepared by a sonochemical method. Mater Sci Semicond Process 16:1109–1116. https://doi.org/10.1016/j.mssp.2013.03.005

Gou J et al (2018) Synthesis of silver/silver chloride/exfoliated graphite nano-photocatalyst and its enhanced visible light photocatalytic mechanism for degradation of organic pollutants. J Ind Eng Chem 59:99–107. https://doi.org/10.1016/j.jiec.2017.10.011

Guan M et al (2013) Vacancy associates promoting solar-driven photocatalytic activity of ultrathin bismuth oxychloride nanosheets. J Am Chem Soc 135:10411–10417. https://doi.org/10.1021/ja402956f

Guo X, Deng D, Tian Q (2017) One pot controllable synthesis of AgCl nanocrystals with different morphology and their photocatalytic activity. Powder Technol 308:206–213. https://doi.org/10.1016/j.powtec.2016.12.006

Hassan MA, Kang J-H, Johar MA, Ha J-S, Ryu S-W (2018) High-performance ZnS/GaN heterostructure photoanode for photoelectrochemical water splitting applications. Acta Mater 146:171–175. https://doi.org/10.1016/j.actamat.2017.12.063

He Z, Kim C, Lin L, Jeon TH, Lin S, Wang X, Choi W (2017) Formation of heterostructures via direct growth CN on h-BN porous nanosheets for metal-free photocatalysis. Nano Energy 42:58–68. https://doi.org/10.1016/j.nanoen.2017.10.043

He C, Bu X, Yang S, He P, Ding G, Xie X (2018) Core–shell $SrTiO_3$/graphene structure by chemical vapor deposition for enhanced photocatalytic performance. Appl Surf Sci 436:373–381. https://doi.org/10.1016/j.apsusc.2017.12.063

Helal A, Harraz FA, Ismail AA, Sami TM, Ibrahim IA (2016) Controlled synthesis of bismuth sulfide nanorods by hydrothermal method and their photocatalytic activity. Mater Des 102:202–212. https://doi.org/10.1016/j.matdes.2016.04.043

Hou H, Peng Q, Zhang S, Guo Q, Xie Y (2005) A "user-friendly" chemical approach towards paramagnetic cobalt phosphide hollow structures: preparation, characterization, and formation mechanism of Co_2P hollow spheres and tubes. Eur J Inorg Chem 2005:2625–2630. https://doi.org/10.1002/ejic.200500033

Hou Z, Chen F, Wang J, François-Xavier CP, Wintgens T (2018) Novel Pd/$GdCrO_3$ composite for photo-catalytic reduction of nitrate to N_2 with high selectivity and activity. Appl Catal B 232:124–134. https://doi.org/10.1016/j.apcatb.2018.03.055

https://www.nature.com/articles/ncomms2818#supplementary-information

https://www.nature.com/articles/ncomms8698#supplementary-information

Hu P, Ngaw CK, Yuan Y, Bassi PS, Joachim Loo SC, Yang Tan TT (2016) Bandgap engineering of ternary sulfide nanocrystals by solution proton alloying for efficient photocatalytic H_2 evolution. Nano Energy 26:577–585. https://doi.org/10.1016/j.nanoen.2016.06.006

Hu Z, Chen D, Wang S, Zhang N, Qin L, Huang Y (2017) Facile synthesis of Sm-doped $BiFeO_3$ nanoparticles for enhanced visible light photocatalytic performance. Mater Sci Eng B 220:1–12. https://doi.org/10.1016/j.mseb.2017.03.005

Huang C et al (2015) Carbon-doped BN nanosheets for metal-free photoredox catalysis. Nat Commun 6:7698. https://doi.org/10.1038/ncomms8698

Hussain W et al (2017) Photocatalytic applications of Cr_2S_3 synthesized from single and multi-source precursors. Mater Chem Phys 194:345–355. https://doi.org/10.1016/j.matchemphys.2017.04.001

Hwang J-S, Chang J-S, Park S-E, Ikeue K, Anpo M (2005) Photoreduction of carbondioxide on surface functionalized nanoporous catalysts. Top Catal 35:311–319. https://doi.org/10.1007/s11244-005-3839-8

Jang JS, Choi SH, Shin N, Yu C, Lee JS (2007) $AgGaS_2$-type photocatalysts for hydrogen production under visible light: effects of post-synthetic H_2S treatment. J Solid State Chem 180:1110–1118. https://doi.org/10.1016/j.jssc.2007.01.008

Jayapandi S, Lakshmi D, Premkumar S, Packiyaraj P, Anitha K (2018) Augmented photocatalytic and electrochemical activities of Ag tailored $LaCoO_3$ perovskite semiconductor. Mater Lett 218:205–208. https://doi.org/10.1016/j.matlet.2018.02.015

Ji Z, Feng L, Kong L, Shen X, Wang J, Xu K, Yue X (2017) Synthesis of GO–$AgIO_4$ nanocomposites with enhanced photocatalytic efficiency in the degradation of organic pollutants. J Mater Sci 52:6100–6110. https://doi.org/10.1007/s10853-017-0849-4

Jiang Z, Pan J, Wang B, Li C (2018) Two dimensional Z-scheme AgCl/Ag/$CaTiO_3$ nano-heterojunctions for photocatalytic hydrogen production enhancement. Appl Surf Sci 436:519–526. https://doi.org/10.1016/j.apsusc.2017.12.065

Jin S, Dong G, Luo J, Ma F, Wang C (2018) Improved photocatalytic NO removal activity of $SrTiO_3$ by using $SrCO_3$ as a new co-catalyst. Appl Catal B 227:24–34. https://doi.org/10.1016/j.apcatb.2018.01.020

Jo W-K, Kim J-T (2009) Application of visible-light photocatalysis with nitrogen-doped or unmodified titanium dioxide for control of indoor-level volatile organic compounds. J Hazard Mater 164:360–366. https://doi.org/10.1016/j.jhazmat.2008.08.033

Kahlon SK, Sharma G, Julka JM, Kumar A, Sharma S, Stadler FJ (2018) Impact of heavy metals and nanoparticles on aquatic biota. Environ Chem Lett. https://doi.org/10.1007/s10311-018-0737-4

Kamata K, Maeda K, Lu D, Kako Y, Domen K (2009) Synthesis and photocatalytic activity of gallium–zinc–indium mixed oxynitride for hydrogen and oxygen evolution under visible light. Chem Phys Lett 470:90–94. https://doi.org/10.1016/j.cplett.2009.01.012

Kandavelu V, Kastien H, Thampi KR (2004) Photocatalytic degradation of isothiazolin-3-ones in water and emulsion paints containing nanocrystalline TiO_2 and ZnO catalysts. Appl Catal B 48:101–111. https://doi.org/10.1016/j.apcatb.2003.09.022

Kane SN, Raghuvanshi S, Satalkar M, Reddy VR, Deshpande UP, Tatarchuk TR, Mazaleyrat F (2018) Synthesis, characterization and antistructure modeling of Ni nano ferrite. AIP Conf Proc 1953:030089. https://doi.org/10.1063/1.5032424

Kang Y, Yang Y, Yin LC, Kang X, Liu G, Cheng HM (2015) An amorphous carbon nitride photocatalyst with greatly extended visible-light-responsive range for photocatalytic hydrogen generation. Adv Mater 27:4572–4577. https://doi.org/10.1002/adma.201501939

Kanhere P, Chen Z (2014) A review on visible light active perovskite-based photocatalysts. Molecules 19:19995–20022. https://doi.org/10.3390/molecules191219995

Kant S, Kalia S, Kumar A (2013) A novel nanocomposite of polyaniline and $Fe_{0.01}Ni_{0.01}Zn_{0.98}O$: photocatalytic, electrical and antibacterial properties. J Alloys Compd 578:249–256. https://doi.org/10.1016/j.jallcom.2013.05.120

Kant S, Pathania D, Singh P, Dhiman P, Kumar A (2014) Removal of malachite green and methylene blue by $Fe_{0.01}Ni_{0.01}Zn_{0.98}O$/polyacrylamide nanocomposite using coupled adsorption and photocatalysis. Appl Catal B 147:340–352. https://doi.org/10.1016/j.apcatb.2013.09.001

Kasahara A, Nukumizu K, Takata T, Kondo JN, Hara M, Kobayashi H, Domen K (2003) $LaTiO_2N$ as a visible-light ($\leq$600 nm)-driven photocatalyst (2). J Phys Chem B 107:791–797. https://doi.org/10.1021/jp026767q

Kawashima K, Hojamberdiev M, Yubuta K, Domen K, Teshima K (2017) Synthesis and visible-light-induced sacrificial photocatalytic water oxidation of quinary oxynitride $BaNb_{0.5}Ta_{0.5}O_2N$ crystals. J Energy. https://doi.org/10.1016/j.jechem.2017.09.006

Kefeni KK, Mamba BB, Msagati TAM (2017) Application of spinel ferrite nanoparticles in water and wastewater treatment: a review. Sep Purif Technol 188:399–422. https://doi.org/10.1016/j.seppur.2017.07.015

Khan MM, Ansari SA, Pradhan D, Ansari MO, Lee J, Cho MH (2014) Band gap engineered TiO_2 nanoparticles for visible light induced photoelectrochemical and photocatalytic studies. J Mater Chem A 2:637–644. https://doi.org/10.1039/C3TA14052K

Khan A, Alam U, Raza W, Bahnemann D, Muneer M (2018) One-pot, self-assembled hydrothermal synthesis of 3D flower-like CuS/g-C_3N_4 composite with enhanced photocatalytic activity under

visible-light irradiation. J Phys Chem Solids 115:59–68. https://doi.org/10.1016/j.jpcs.2017.10.032
Kim YK, Park H (2011) Light-harvesting multi-walled carbon nanotubes and CdS hybrids: application to photocatalytic hydrogen production from water. Energy Environ Sci 4:685–694. https://doi.org/10.1039/C0EE00330A
Kim J, Hwang DW, Kim HG, Bae SW, Lee JS, Li W, Oh SH (2005) Highly efficient overall water splitting through optimization of preparation and operation conditions of layered perovskite photocatalysts. Top Catal 35:295–303. https://doi.org/10.1007/s11244-005-3837-x
Kim HG, Borse PH, Jang JS, Jeong ED, Jung O-S, Suh YJ, Lee JS (2009) Fabrication of $CaFe_2O_4/MgFe_2O_4$ bulk heterojunction for enhanced visible light photocatalysis. Chem Commun. https://doi.org/10.1039/B911805E
Kim H, Choi Y, Hu S, Choi W, Kim J-H (2018) Photocatalytic hydrogen peroxide production by anthraquinone-augmented polymeric carbon nitride. Appl Catal B Environ 229:121–129. https://doi.org/10.1016/j.apcatb.2018.01.060
Kitano M, Matsuoka M, Ueshima M, Anpo M (2007) Recent developments in titanium oxide-based photocatalysts. Appl Catal A 325:1–14. https://doi.org/10.1016/j.apcata.2007.03.013
Kobayashi B, Ohkita H, Mizushima T, Kakuta N (2014) Preparation of tabular silver bromide and its photocatalytic performance. Catal Commun 45:21–24. https://doi.org/10.1016/j.catcom.2013.10.023
Kondo A, Yin G, Srinivasan N, Atarashi D, Sakai E, Miyauchi M (2015) Kelvin probe imaging of photo-injected electrons in metal oxide nanosheets from metal sulfide quantum dots under remote photochromic coloration. Nanoscale 7:12510–12515. https://doi.org/10.1039/C5NR02405F
Kudo A (2006) Development of photocatalyst materials for water splitting. Int J Hydrogen Energy 31:197–202. https://doi.org/10.1016/j.ijhydene.2005.04.050
Kudo A, Miseki Y (2009) Heterogeneous photocatalyst materials for water splitting. Chem Soc Rev 38:253–278. https://doi.org/10.1039/B800489G
Kumar A, Sharma G, Naushad M, Singh P, Kalia S (2014) Polyacrylamide/$Ni_{0.02}Zn_{0.98}O$ nanocomposite with high solar light photocatalytic activity and efficient adsorption capacity for toxic dye removal. Ind Eng Chem Res 53:15549–15560. https://doi.org/10.1021/ie5018173
Kumar A, Sharma G, Naushad M, Thakur S (2015) SPION/β-cyclodextrin core–shell nanostructures for oil spill remediation and organic pollutant removal from waste water. Chem Eng J 280:175–187. https://doi.org/10.1016/j.cej.2015.05.126
Kumar A, Guo C, Sharma G, Pathania D, Naushad M, Kalia S, Dhiman P (2016) Magnetically recoverable ZrO_2/Fe_3O_4/chitosan nanomaterials for enhanced sunlight driven photoreduction of carcinogenic Cr(VI) and dechlorination and mineralization of 4-chlorophenol from simulated waste water. RSC Adv 6:13251–13263. https://doi.org/10.1039/C5RA23372K
Kumar A et al (2017a) Solar-driven photodegradation of 17-β-estradiol and ciprofloxacin from waste water and CO_2 conversion using sustainable coal-char/polymeric-gC_3N_4/RGO metal-free nanohybrids. New J Chem 41:10208–10224
Kumar A et al (2017b) ZnSe-WO_3 nano-hetero-assembly stacked on Gum ghatti for photo-degradative removal of bisphenol A: Symbiose of adsorption and photocatalysis. Int J Biol Macromol 104:1172–1184. https://doi.org/10.1016/j.ijbiomac.2017.06.116
Kumar A et al (2018a) Biochar-templated g-$C_3N_4/Bi_2O_2CO_3/CoFe_2O_4$ nano-assembly for visible and solar assisted photo-degradation of paraquat, nitrophenol reduction and CO_2 conversion. Chem Eng J 339:393–410. https://doi.org/10.1016/j.cej.2018.01.105
Kumar A, Kumar A, Sharma G, Al-Muhtaseb AAH, Naushad M, Ghfar AA, Stadler FJ (2018b) Quaternary magnetic BiOCl/g-$C_3N_4/Cu_2O/Fe_3O_4$ nano-junction for visible light and solar powered degradation of sulfamethoxazole from aqueous environment. Chem Eng J 334:462–478. https://doi.org/10.1016/j.cej.2017.10.049
Kumar A et al (2018c) Aerogels and metal–organic frameworks for environmental remediation and energy production. Environ Chem Lett. https://doi.org/10.1039/C7NJ01580A
Lee Y-K, Oyama ST (2006) Bifunctional nature of a SiO_2-supported Ni_2P catalyst for hydrotreating: EXAFS and FTIR studies. J Catal 239:376–389. https://doi.org/10.1016/j.jcat.2005.12.029
Lee TH, Kim SY, Jang HW (2016) Black phosphorus: critical review and potential for water splitting photocatalyst. Nanomaterials 6:194. https://doi.org/10.3390/nano6110194
Lei W, Portehault D, Liu D, Qin S, Chen Y (2013) Porous boron nitride nanosheets for effective water cleaning. Nat Commun 4:1777. https://doi.org/10.1038/ncomms2818
Li D, Haneda H (2003) Synthesis of nitrogen-containing ZnO powders by spray pyrolysis and their visible-light photocatalysis in gas-phase acetaldehyde decomposition. J Photochem Photobiol A 155:171–178. https://doi.org/10.1016/S1010-6030(02)00371-4
Li D, Haneda H, Ohashi N, Hishita S, Yoshikawa Y (2004) Synthesis of nanosized nitrogen-containing MO_X–ZnO (M = W, V, Fe) composite powders by spray pyrolysis and their visible-light-driven photocatalysis in gas-phase acetaldehyde decomposition. Catal Today 93–95:895–901. https://doi.org/10.1016/j.cattod.2004.06.099
Li D, Haneda H, Ohashi N, Saito N, Hishita S (2005a) Morphological reform of ZnO particles induced by coupling with MO_x (M = V, W, Ce) and the effects on photocatalytic activity. Thin Solid Films 486:20–23. https://doi.org/10.1016/j.tsf.2004.11.237
Li Y, Malik MA, O'Brien P (2005b) Synthesis of single-crystalline CoP nanowires by a one-pot metal–organic route. J Am Chem Soc 127:16020–16021. https://doi.org/10.1021/ja055963i
Li G, Kako T, Wang D, Zou Z, Ye J (2009a) Enhanced photocatalytic activity of La-doped $AgNbO_3$ under visible light irradiation. Dalton Trans 13:2423–2427
Li J, Ni Y, Liao K, Hong J (2009b) Hydrothermal synthesis of $Ni_{12}P_5$ hollow microspheres, characterization and photocatalytic degradation property. J Colloid Interface Sci 332:231–236. https://doi.org/10.1016/j.jcis.2008.12.058
Li L, Zhang Y, Schultz AM, Liu X, Salvador PA, Rohrer GS (2012) Visible light photochemical activity of heterostructured $PbTiO_3$–TiO_2 core–shell particles. Catal Sci Technol 2:1945–1952. https://doi.org/10.1039/C2CY20202F
Li J, Yu Y, Zhang L (2014) Bismuth oxyhalide nanomaterials: layered structures meet photocatalysis. Nanoscale 6:8473–8488. https://doi.org/10.1039/C4NR02553A
Li Q, Zhao X, Yang J, Jia C-J, Jin Z, Fan W (2015a) Exploring the effects of nanocrystal facet orientations in g-C_3N_4/BiOCl heterostructures on photocatalytic performance. Nanoscale 7:18971–18983. https://doi.org/10.1039/c5nr05154a
Li Y, Cheng X, Ruan X, Song H, Lou Z, Ye Z, Zhu L (2015b) Enhancing photocatalytic activity for visible-light-driven H_2 generation with the surface reconstructed $LaTiO_2N$ nanostructures. Nano Energy 12:775–784. https://doi.org/10.1016/j.nanoen.2015.02.003
Li J, Li J, Zhou X, Xia Z, Gao W, Ma Y, Qu Y (2016a) Highly efficient and robust nickel phosphides as bifunctional electrocatalysts for overall water-splitting. ACS Appl Mater Interfaces 8:10826–10834. https://doi.org/10.1021/acsami.6b00731
Li Y et al (2016b) In situ loading of Ag_2WO_4 on ultrathin g-C_3N_4 nanosheets with highly enhanced photocatalytic performance. J Hazard Mater 313:219–228. https://doi.org/10.1016/j.jhazmat.2016.04.011

Li M et al (2017a) Core–shell $LaPO_4$/g-C_3N_4 nanowires for highly active and selective CO_2 reduction. Appl Catal B 201:629–635. https://doi.org/10.1016/j.apcatb.2016.09.004

Li X, Zhang H, Huang J, Luo J, Feng Z, Wang X (2017b) Folded nano-porous graphene-like carbon nitride with significantly improved visible-light photocatalytic activity for dye degradation. Ceram Int 43:15785–15792. https://doi.org/10.1016/j.ceramint.2017.08.144

Li Z, Ai J, Ge M (2017c) A facile approach assembled magnetic $CoFe_2O_4$/AgBr composite for dye degradation under visible light. J Environ Chem Eng 5:1394–1403. https://doi.org/10.1016/j.jece.2017.02.024

Li H et al (2018a) Conjugated polyene-functionalized graphitic carbon nitride with enhanced photocatalytic water-splitting efficiency. Carbon 129:637–645. https://doi.org/10.1016/j.carbon.2017.12.048

Li R et al (2018b) Iodide-modified $Bi_4O_5Br_2$ photocatalyst with tunable conduction band position for efficient visible-light decontamination of pollutants. Chem Eng J 339:42–50. https://doi.org/10.1016/j.cej.2018.01.109

Lin K-S, Adhikari AK, Tsai Z-Y, Chen Y-P, Chien T-T, Tsai H-B (2011) Synthesis and characterization of nickel ferrite nanocatalysts for CO_2 decomposition. Catal Today 174:88–96. https://doi.org/10.1016/j.cattod.2011.02.013

Liu J, Zhang Y, Lu L, Wu G, Chen W (2012) Self-regenerated solar-driven photocatalytic water-splitting by urea derived graphitic carbon nitride with platinum nanoparticles. Chem Commun 48:8826–8828. https://doi.org/10.1039/C2CC33644H

Liu C et al (2017a) Explore the properties and photocatalytic performance of iron-doped g-C_3N_4 nanosheets decorated with Ni_2P. Mol Catalysis 437:80–88. https://doi.org/10.1016/j.mcat.2017.02.038

Liu D, Zhang M, Xie W, Sun L, Chen Y, Lei W (2017b) Porous BN/TiO_2 hybrid nanosheets as highly efficient visible-light-driven photocatalysts. Appl Catal B 207:72–78. https://doi.org/10.1016/j.apcatb.2017.02.011

Liu J et al (2017c) Graphene quantum dots modified mesoporous graphite carbon nitride with significant enhancement of photocatalytic activity. Appl Catal B 207:429–437. https://doi.org/10.1016/j.apcatb.2017.01.071

Liu Y et al (2018) Facet and morphology dependent photocatalytic hydrogen evolution with CdS nanoflowers using a novel mixed solvothermal strategy. J Colloid Interface Sci 513:222–230. https://doi.org/10.1016/j.jcis.2017.11.030

Logvinovich D, Ebbinghaus Stefan G, Reller A, Marozau I, Ferri D, Weidenkaff A (2010) Synthesis, crystal structure and optical properties of $LaNbON_2$. Zeitschrift für anorganische und allgemeine Chemie 636:905–912. https://doi.org/10.1002/zaac.201000067

Lu M, Yuan G, Wang Z, Wang Y, Guo J (2015) Synthesis of $BiPO_4$/Bi_2S_3 heterojunction with enhanced photocatalytic activity under visible-light irradiation. Nanoscale Res Lett 10:385. https://doi.org/10.1186/s11671-015-1092-z

Lu K-Q, Yuan L, Xin X, Xu Y-J (2018a) Hybridization of graphene oxide with commercial graphene for constructing 3D metal-free aerogel with enhanced photocatalysis. Appl Catal B 226:16–22. https://doi.org/10.1016/j.apcatb.2017.12.032

Lu Y, Ji C, Li Y, Qu R, Sun C, Zhang Y (2018b) Facile one-pot synthesis of C and g-C_3N_4 composites with enhanced photocatalytic activity using hydroxymethylated melamine as carbon source and soft template. Mater Lett 211:78–81. https://doi.org/10.1016/j.matlet.2017.09.080

Lv J, Liu J, Zhang J, Dai K, Liang C, Wang Z, Zhu G (2018) Construction of organic–inorganic cadmium sulfide/diethylenetriamine hybrids for efficient photocatalytic hydrogen production. J Colloid Interface Sci 512:77–85. https://doi.org/10.1016/j.jcis.2017.10.052

Maeda K, Domen K (2007) New non-oxide photocatalysts designed for overall water splitting under visible light. J Phys Chem C 111:7851–7861. https://doi.org/10.1021/jp070911w

Maensiri S, Sangmanee M, Wiengmoon A (2009) Magnesium ferrite nanostructures fabricated by electrospinning. Nanoscale Res Lett 4:221. https://doi.org/10.1007/s11671-008-9229-y

Mane D, Birajdar D, Patil S, Shirsath SE, Kadam R (2011) Redistribution of cations and enhancement in magnetic properties of sol–gel synthesized $Cu_{0.7-x}Co_xZn_{0.3}Fe_2O_4$ ($0 \le x \le 0.5$). J Sol Gel Sci Technol 58:70–79. https://doi.org/10.1007/s10971-010-2357-8

Mera AC, Moreno Y, Contreras D, Escalona N, Meléndrez MF, Mangalaraja RV, Mansilla HD (2017) Improvement of the BiOI photocatalytic activity optimizing the solvothermal synthesis. Solid State Sci 63:84–92. https://doi.org/10.1016/j.solidstatesciences.2016.11.013

Mi K, Ni Y, Hong J (2011) Solvent-controlled syntheses of $Ni_{12}P_5$ and Ni_2P nanocrystals and photocatalytic property comparison. J Phys Chem Solids 72:1452–1456. https://doi.org/10.1016/j.jpcs.2011.08.028

Mi L, Huang Y, Qin L, Seo HJ (2018) Improved photo-degradation of dyes over Ag-loaded $NiTiO_3$:V nanorods on visible-light-irradiation. Mater Res Bull 102:269–276. https://doi.org/10.1016/j.materresbull.2018.02.043

Mishra D, Senapati KK, Borgohain C, Perumal A (2012) $CoFe_2O_4$–Fe_3O_4 magnetic nanocomposites as photocatalyst for the degradation of methyl orange dye. J Nanotechnol. https://doi.org/10.1155/2012/323145

Miyauchi M, Nakajima A, Watanabe T, Hashimoto K (2002) Photocatalysis and photoinduced hydrophilicity of various metal oxide thin films. Chem Mater 14:2812–2816. https://doi.org/10.1021/cm020076p

Moniruddin M et al (2018) Recent progress on perovskite materials in photovoltaic and water splitting applications. Mater Today Energy 7:246–259. https://doi.org/10.1016/j.mtener.2017.10.005

Naushad M et al (2018) Efficient removal of toxic phosphate anions from aqueous environment using pectin based quaternary amino anion exchanger. Int J Biol Macromol 106:1–10. https://doi.org/10.1016/j.ijbiomac.2017.07.169

Ni Y, Li J, Zhang L, Yang S, Wei X (2009) Urchin-like Co_2P nanocrystals: synthesis, characterization, influencing factors and photocatalytic degradation property. Mater Res Bull 44:1166–1172. https://doi.org/10.1016/j.materresbull.2008.09.041

Ni L, Tanabe M, Irie H (2013) A visible-light-induced overall water-splitting photocatalyst: conduction-band-controlled silver tantalate. Chem Commun 49:10094–10096. https://doi.org/10.1039/C3CC45222K

Nuraje N, Su K (2013) Perovskite ferroelectric nanomaterials. Nanoscale 5:8752–8780. https://doi.org/10.1039/C3NR02543H

Nurlaela E, Ziani A, Takanabe K (2016) Tantalum nitride for photocatalytic water splitting: concept and applications. Mater Renew Sustain Energy 5:18. https://doi.org/10.1007/s40243-016-0083-z

Ogo Y, Hiramatsu H, Nomura K, Yanagi H, Kamiya T, Hirano M, Hosono H (2008) p-Channel thin-film transistor using *p*-type oxide semiconductor, SnO. Appl Phys Lett 93:032113. https://doi.org/10.1063/1.2964197

Ong CB, Ng LY, Mohammad AW (2018) A review of ZnO nanoparticles as solar photocatalysts: synthesis, mechanisms and applications. Renew Sustain Energy Rev 81:536–551. https://doi.org/10.1016/j.rser.2017.08.020

Osterloh FE (2007) Inorganic materials as catalysts for photochemical splitting of water. Chem Mater 20:35–54. https://doi.org/10.1021/cm7024203

Pan Z, Wang R, Li J, Iqbal S, Liu W, Zhou K (2018) Fe_2P nanoparticles as highly efficient freestanding co-catalyst for

photocatalytic hydrogen evolution. Int J Hydrogen Energy 43:5337–5345. https://doi.org/10.1016/j.ijhydene.2017.09.128

Preethi G, Ninan AS, Kumar K, Balan R, Nagaswarupa HP (2017) Molten salt synthesis of nanocrystalline $ZnFe_2O_4$ and its photocatalytic dye degradation studies. Mater Today Proc 4:11816–11819. https://doi.org/10.1016/j.matpr.2017.09.099

Qiu P, Xu C, Zhou N, Chen H, Jiang F (2018) Metal-free black phosphorus nanosheets-decorated graphitic carbon nitride nanosheets with CP bonds for excellent photocatalytic nitrogen fixation. Appl Catal B 221:27–35. https://doi.org/10.1016/j.apcatb.2017.09.010

Qu Y, Zhou W, Ren Z, Du S, Meng X, Tian G, Pan K, Wang G, Fu H (2012) Facile preparation of porous $NiTiO_3$ nanorods with enhanced visible-light-driven photocatalytic performance. J Mater Chem 22(32):16471

Qu Y, Zhou W, Fu H (2014) Porous cobalt titanate nanorod: a new candidate for visible light-driven photocatalytic water oxidation. ChemCatChem 6:265–270. https://doi.org/10.1002/cctc.201300718

Raghuvanshi S, Kane SN, Tatarchuk TR, Mazaleyrat F (2018) Effect of Zn addition on structural, magnetic properties, antistructural modeling of $Co_{1-x}Zn_xFe_2O_4$ nano ferrite. AIP Conf Proc 1953:030055. https://doi.org/10.1063/1.5032390

Rashmi SK, Bhojya Naik HS, Jayadevappa H, Viswanath R, Patil SB, Madhukara Naik M (2017) Solar light responsive Sm-Zn ferrite nanoparticle as efficient photocatalyst. Mater Sci Eng B 225:86–97. https://doi.org/10.1016/j.mseb.2017.08.012

Rekhila G, Bessekhouad Y, Trari M (2016) Synthesis and characterization of the spinel $ZnFe_2O_4$, application to the chromate reduction under visible light. Environ Technol Innov 5:127–135. https://doi.org/10.1016/j.eti.2016.01.007

Ren A, Liu C, Hong Y, Shi W, Lin S, Li P (2014) Enhanced visible-light-driven photocatalytic activity for antibiotic degradation using magnetic $NiFe_2O_4/Bi_2O_3$ heterostructures. Chem Eng J 258:301–308. https://doi.org/10.1016/j.cej.2014.07.071

Ren Z et al (2017) Carbon quantum dots decorated $MoSe_2$ photocatalyst for Cr(VI) reduction in the UV–Vis–NIR photon energy range. J Colloid Interface Sci 488:190–195. https://doi.org/10.1016/j.jcis.2016.10.077

Romero M, Blanco J, Sánchez B, Vidal A, Sixto M, Cardona AI, Garcia E (1999) Solar photocatalytic degradation of water and air pollutants: challenges and perspectives. Sol Energy 66:169–182. https://doi.org/10.1016/S0038-092X(98)00120-0

Saeed M, Ahmad A, Boddula R, ul Haq A, Azhar A (2018) Ag@Mn_xO_y: an effective catalyst for photo-degradation of rhodamine B dye. Environ Chem Lett 16:287–294. https://doi.org/10.1007/s10311-017-0661-z

Sanz J, Lombrana J, De Luis A, Ortueta M, Varona F (2003) Microwave and Fenton's reagent oxidation of wastewater. Environ Chem Lett 1:45–50. https://doi.org/10.1007/s10311-002-0007-2

Satalkar M, Kane SN, Tatarchuk T, Araújo JP (2018) Ni addition induced changes in structural, magnetic, and cationic distribution of $Zn_{0.75-x}Ni_xMg_{0.15}Cu_{0.1}Fe_2O_4$ nano-ferrite. In: Fesenko O, Yatsenko L (eds) Nanochemistry, biotechnology, nanomaterials, and their applications. Springer, Cham, pp 357–375. https://doi.org/10.1007/978-3-319-92567-7_23

Sathish M, Viswanathan B, Viswanath RP (2006) Alternate synthetic strategy for the preparation of CdS nanoparticles and its exploitation for water splitting. Int J Hydrogen Energy 31:891–898. https://doi.org/10.1016/j.ijhydene.2005.08.002

Serpone N, Khairutdinov RF (1997) Application of nanoparticles in the photocatalytic degradation of water pollutants. In: Kamat PV, Meisel D (eds) Studies in surface science and catalysis, vol 103. Elsevier, New York, pp 417–444. https://doi.org/10.1016/S0167-2991(97)81113-5

Sfaelou S, Lianos P (2016) Photoactivated fuel cells (PhotoFuelCells). An alternative source of renewable energy with environmental benefits. AIMS Mater Sci 3:270–288. https://doi.org/10.3934/matersci.2016.1.270

Shamraiz U, Hussain RA, Badshah A, Raza B, Saba S (2016) Functional metal sulfides and selenides for the removal of hazardous dyes from water. J Photochem Photobiol B 159:33–41. https://doi.org/10.1016/j.jphotobiol.2016.03.013

Shangguan W, Yoshida A (2002) Photocatalytic hydrogen evolution from water on nanocomposites incorporating cadmium sulfide into the interlayer. J Phys Chem B 106:12227–12230. https://doi.org/10.1021/jp0212500

Sharma K, Kumar V, Kaith BS, Kumar V, Som S, Kalia S, Swart HC (2015) Synthesis, characterization and water retention study of biodegradable Gum ghatti-poly(acrylic acid–aniline) hydrogels. Polym Degrad Stab 111:20–31. https://doi.org/10.1016/j.polymdegradstab.2014.10.012

Sharma G, Gupta VK, Agarwal S, Kumar A, Thakur S, Pathania D (2016a) Fabrication and characterization of Fe@MoPO nanoparticles: ion exchange behavior and photocatalytic activity against malachite green. J Mol Liq 219:1137–1143. https://doi.org/10.1016/j.molliq.2016.04.046

Sharma G, Naushad M, Pathania D, Kumar A (2016b) A multifunctional nanocomposite pectin thorium(IV) tungstomolybdate for heavy metal separation and photoremediation of malachite green. Desalin Water Treat 57:19443–19455. https://doi.org/10.1080/19443994.2015.1096834

Sharma G, ALOthman ZA, Kumar A, Sharma S, Ponnusamy SK, Naushad M (2017a) Fabrication and characterization of a nanocomposite hydrogel for combined photocatalytic degradation of a mixture of malachite green and fast green dye. Nanotechnol Environ Eng 2:4. https://doi.org/10.1007/s41204-017-0014-y

Sharma G, Bhogal S, Naushad M, Inamuddin, Kumar A, Stadler FJ (2017b) Microwave assisted fabrication of La/Cu/Zr/carbon dots trimetallic nanocomposites with their adsorptional vs photocatalytic efficiency for remediation of persistent organic pollutants. J Photochem Photobiol A 347:235–243. https://doi.org/10.1016/j.jphotochem.2017.07.001

Sharma G, Kumar A, Chauhan C, Okram A, Sharma S, Pathania D, Kalia S (2017c) Pectin-crosslinked-guar gum/SPION nanocomposite hydrogel for adsorption of m-cresol and o-chlorophenol. Sustain Chem Pharm 6:96–106. https://doi.org/10.1016/j.scp.2017.10.003

Sharma G et al (2017d) Efficient removal of coomassie brilliant blue R-250 dye using starch/poly(alginic acid-cl-acrylamide) nanohydrogel. Process Saf Environ Prot 109:301–310. https://doi.org/10.1016/j.psep.2017.04.011

Sharma G, Thakur B, Naushad M, Al-Muhtaseb AAH, Kumar A, Sillanpaa M, Mola GT (2017e) Fabrication and characterization of sodium dodecyl sulphate@ironsilicophosphate nanocomposite: ion exchange properties and selectivity for binary metal ions. Mater Chem Phys 193:129–139. https://doi.org/10.1016/j.matchemphys.2017.02.010

Sharma G et al (2018a) Guar gum-crosslinked-Soya lecithin nanohydrogel sheets as effective adsorbent for the removal of thiophanate methyl fungicide. Int J Biol Macromol 114:295–305. https://doi.org/10.1016/j.ijbiomac.2018.03.093

Sharma G et al (2018b) Photoremediation of toxic dye from aqueous environment using monometallic and bimetallic quantum dots based nanocomposites. J Clean Prod 172:2919–2930. https://doi.org/10.1016/j.jclepro.2017.11.122

Sharma G, Thakur B, Naushad M, Kumar A, Stadler FJ, Alfadul SM, Mola GT (2018c) Applications of nanocomposite hydrogels for biomedical engineering and environmental protection. Environ Chem Lett 16:113–146. https://doi.org/10.1007/s10311-017-0671-x

Shen Q, Arae D, Toyoda T (2004) Photosensitization of nanostructured TiO_2 with CdSe quantum dots: effects of microstructure and electron transport in TiO_2 substrates. J Photochem Photobiol A 164:75–80. https://doi.org/10.1016/j.jphotochem.2003.12.027

Shen S, Zhao L, Guo L (2009) Crystallite, optical and photocatalytic properties of visible-light-driven $ZnIn_2S_4$ photocatalysts synthesized via a surfactant-assisted hydrothermal method. Mater Res Bull 44:100–105. https://doi.org/10.1016/j.materresbull.2008.03.027

Shi L et al (2016) *n*-Type boron phosphide as a highly stable, metal-free, visible-light-active photocatalyst for hydrogen evolution. Nano Energy 28:158–163. https://doi.org/10.1016/j.nanoen.2016.08.041

Shiraishi Y, Kanazawa S, Sugano Y, Tsukamoto D, Sakamoto H, Ichikawa S, Hirai T (2014) Highly selective production of hydrogen peroxide on graphitic carbon nitride ($g\text{-}C_3N_4$) photocatalyst activated by visible light. ACS Catal 4:774–780. https://doi.org/10.1021/cs401208c

Singh P, Raizada P, Kumari S, Kumar A, Pathania D, Thakur P (2014) Solar-Fenton removal of malachite green with novel Fe^0-activated carbon nanocomposite. Appl Catal A 476:9–18. https://doi.org/10.1016/j.apcata.2014.02.009

Sinha ASK, Sahu N, Arora MK, Upadhyay SN (2001) Preparation of egg-shell type Al_2O_3-supported CdS photocatalysts for reduction of H_2O to H_2. Catal Today 69:297–305. https://doi.org/10.1016/S0920-5861(01)00382-0

Sivaprakash K, Induja M, Gomathi Priya P (2018) Facile synthesis of metal free non-toxic boron carbon nitride nanosheets with strong photocatalytic behavior for degradation of industrial dyes. Mater Res Bull 100:313–321. https://doi.org/10.1016/j.materresbull.2017.12.039

Song L, Zhang S (2018) A novel cocatalyst of NiCoP significantly enhances visible-light photocatalytic hydrogen evolution over cadmium sulfide. J Ind Eng Chem 61:197–205. https://doi.org/10.1016/j.jiec.2017.12.017

Song H, Peng T, Cai P, Yi H, Yan C (2007) Hydrothermal synthesis of flaky crystallized $La_2Ti_2O_7$ for producing hydrogen from photocatalytic water splitting. Catal Lett 113:54–58. https://doi.org/10.1007/s10562-006-9004-6

Song X, Shen W, Sun Z, Yang C, Zhang P, Gao L (2016) Size-engineerable NiS_2 hollow spheres photo co-catalysts from supermolecular precursor for H_2 production from water splitting. Chem Eng J 290:74–81. https://doi.org/10.1016/j.cej.2016.01.030

Srinivasan N, Shiga Y, Atarashi D, Sakai E, Miyauchi M (2015) A PEDOT-coated quantum dot as efficient visible light harvester for photocatalytic hydrogen production. Appl Catal B 179:113–121. https://doi.org/10.1016/j.apcatb.2015.05.007

Stampfl C, Freeman AJ (2005) Stable and metastable structures of the multiphase tantalum nitride system. Phys Rev B 71:024111. https://doi.org/10.1103/PhysRevB.71.024111

Su T, Qin Z, Ji H, Jiang Y, Huang G (2016) Recent advances in the photocatalytic reduction of carbon dioxide. Environ Chem Lett 14:99–112. https://doi.org/10.1007/s10311-018-0729-4

Sun S, Yang X, Zhang Y, Zhang F, Ding J, Bao J, Gao C (2012) Enhanced photocatalytic activity of sponge-like $ZnFe_2O_4$ synthesized by solution combustion method. Prog Nat Sci Mater Int 22:639–643. https://doi.org/10.1016/j.pnsc.2012.11.008

Sun B, Qiao Z, Shang K, Fan H, Ai S (2013) Facile synthesis of silver sulfide/bismuth sulfide nanocomposites for photocatalytic inactivation of *Escherichia coli* under solar light irradiation. Mater Lett 91:142–145. https://doi.org/10.1016/j.matlet.2012.09.074

Sun J, Duan L, Wu Q, Yao W (2018) Synthesis of MoS_2 quantum dots cocatalysts and their efficient photocatalytic performance for hydrogen evolution. Chem Eng J 332:449–455. https://doi.org/10.1016/j.cej.2017.09.026

Surendhiran D, Sirajunnisa A, Tamilselvam K (2017) Silver–magnetic nanocomposites for water purification. Environ Chem Lett 15:367–386. https://doi.org/10.1007/s10311-017-0635-1

Tahir B, Tahir M, Amin NAS (2017) Photo-induced CO_2 reduction by CH_4/H_2O to fuels over Cu-modified $g\text{-}C_3N_4$ nanorods under simulated solar energy. Appl Surf Sci 419:875–885. https://doi.org/10.1016/j.apsusc.2017.05.117

Takahashi H, Igawa K, Arii K, Kamihara Y, Hirano M, Hosono H (2008) Superconductivity at 43 K in an iron-based layered compound $LaO_{1-x}F_x$ FeAs. Nature 453:376. https://doi.org/10.1038/nature06972

Takata T, Pan C, Domen K (2015) Recent progress in oxynitride photocatalysts for visible-light-driven water splitting. Sci Technol Adv Mater 16:033506. https://doi.org/10.1088/1468-6996/16/3/033506

Tang J, Durrant JR, Klug DR (2008) Mechanism of photocatalytic water splitting in TiO_2. Reaction of water with photoholes, importance of charge carrier dynamics, and evidence for four-hole chemistry. J Am Chem Soc 130:13885–13891. https://doi.org/10.1021/ja8034637

Tang L et al (2017) Fabrication of compressible and recyclable macroscopic $g\text{-}C_3N_4$/GO aerogel hybrids for visible-light harvesting: a promising strategy for water remediation. Appl Catal B 219:241–248. https://doi.org/10.1016/j.apcatb.2017.07.053

Tatarchuk T, Bououdina M, Judith Vijaya J, John Kennedy L (2017) Spinel ferrite nanoparticles: synthesis, crystal structure, properties, and perspective applications. In: Fesenko O, Yatsenko L (eds) Nanophysics, nanomaterials, interface studies, and applications. Springer, Cham, pp 305–325. https://doi.org/10.1007/978-3-319-56422-7_22

Tian B, Dong R, Zhang J, Bao S, Yang F, Zhang J (2014) Sandwich-structured AgCl@Ag@TiO_2 with excellent visible-light photocatalytic activity for organic pollutant degradation and *E. coli* K12 inactivation. Appl Catal B 158–159:76–84. https://doi.org/10.1016/j.apcatb.2014.04.008

Tijare S, Bakardjieva S, Subrt J, Joshi M, Rayalu S, Hishita S, Labhsetwar N (2014) Synthesis and visible light photocatalytic activity of nanocrystalline $PrFeO_3$ perovskite for hydrogen generation in ethanol–water system. J Chem Sci 126:517–525. https://doi.org/10.1007/s12039-014-0596-x

Townsend TK, Browning ND, Osterloh FE (2012) Overall photocatalytic water splitting with NiO_x–$SrTiO_3$: a revised mechanism. Energy Environ Sci 5:9543–9550. https://doi.org/10.1039/C2EE22665K

Vance CC, Vaddiraju S, Karthikeyan R (2018) Water disinfection using zinc phosphide nanowires under visible light conditions. J Environ Chem Eng 6:568–573. https://doi.org/10.1016/j.jece.2017.12.052

Vogel R, Hoyer P, Weller H (1994) Quantum-sized PbS, CdS, Ag_2S, Sb_2S_3, and Bi_2S_3 particles as sensitizers for various nanoporous wide-bandgap semiconductors. J Phys Chem 98:3183–3188. https://doi.org/10.1021/j100063a022

Wang C, Shao C, Liu Y, Zhang L (2008) Photocatalytic properties BiOCl and Bi_2O_3 nanofibers prepared by electrospinning. Scr Mater 59:332–335. https://doi.org/10.1016/j.scriptamat.2008.03.038

Wang X et al (2009) A metal-free polymeric photocatalyst for hydrogen production from water under visible light. Nat Mater 8:76. https://doi.org/10.1038/nmat2317

Wang M, Li M, Xu L, Wang L, Ju Z, Li G, Qian Y (2011) High yield synthesis of novel boron nitride submicro-boxes and their photocatalytic application under visible light irradiation. Catal Sci Technol 1:1159–1165. https://doi.org/10.1039/C1CY00111F

Wang R, Zhu Y, Qiu Y, Leung C-F, He J, Liu G, Lau T-C (2013) Synthesis of nitrogen-doped $KNbO_3$ nanocubes with high photocatalytic activity for water splitting and degradation of organic

pollutants under visible light. Chem Eng J 226:123–130. https://doi.org/10.1016/j.cej.2013.04.049
Wang J, Wang X, Liu B, Li X, Cao M (2015a) Facile synthesis of $SrNbO_2N$ nanoparticles with excellent visible-light photocatalytic performances. Mater Lett 152:131–134. https://doi.org/10.1016/j.matlet.2015.03.104
Wang W, Tadé MO, Shao Z (2015b) Research progress of perovskite materials in photocatalysis- and photovoltaics-related energy conversion and environmental treatment. Chem Soc Rev 44:5371–5408. https://doi.org/10.1039/C5CS00113G
Wang AN, Teng Y, Hu X-F, Wu L-H, Huang Y-J, Luo Y-M, Christie P (2016) Diphenylarsinic acid contaminated soil remediation by titanium dioxide (P25) photocatalysis: degradation pathway, optimization of operating parameters and effects of soil properties. Sci Total Environ 541:348–355. https://doi.org/10.1016/j.scitotenv.2015.09.023
Wang S, Guan Y, Lu L, Shi Z, Yan S, Zou Z (2018a) Effective separation and transfer of carriers into the redox sites on Ta_3N_5/Bi photocatalyst for promoting conversion of CO_2 into CH_4. Appl Catal B 224:10–16. https://doi.org/10.1016/j.apcatb.2017.10.043
Wang X-J et al (2018b) Metalloid Ni_2P and its behavior for boosting the photocatalytic hydrogen evolution of $CaIn_2S_4$. Int J Hydrogen Energy 43:219–228. https://doi.org/10.1016/j.ijhydene.2017.11.042
Wang Y et al (2018c) One-pot synthesis of K-doped g-C_3N_4 nanosheets with enhanced photocatalytic hydrogen production under visible-light irradiation. Appl Surf Sci 440:258–265. https://doi.org/10.1016/j.apsusc.2018.01.091
Wang Z, Huo Y, Fan Y, Wu R, Wu H, Wang F, Xu X (2018d) Facile synthesis of carbon-rich g-C_3N_4 by copolymerization of urea and tetracyanoethylene for photocatalytic degradation of Orange II. J Photochem Photobiol A 358:61–69. https://doi.org/10.1016/j.jphotochem.2018.02.036
Weidenkaff A (2004) Preparation and application of nanostructured perovskite phases. Adv Eng Mater 6:709–714. https://doi.org/10.1002/adem.200400098
Weller T, Specht L, Marschall R (2017) Single crystal $CsTaWO_6$ nanoparticles for photocatalytic hydrogen production. Nano Energy 31:551–559. https://doi.org/10.1016/j.nanoen.2016.12.003
Weng Y-C, Chou Y-D, Chang C-J, Chan C-C, Chen K-Y, Su Y-F (2014) Screening of ZnS-based photocatalysts by scanning electrochemical microscopy and characterization of potential photocatalysts. Electrochim Acta 125:354–361. https://doi.org/10.1016/j.electacta.2014.01.127
Wu D, Ye L, Yip HY, Wong PK (2017) Organic-free synthesis of 001 facet dominated BiOBr nanosheets for selective photoreduction of CO_2 to CO Catalysis. Sci Technol 7:265–271. https://doi.org/10.1039/C6CY02040B
Xiao J, Xie Y, Nawaz F, Wang Y, Du P, Cao H (2016) Dramatic coupling of visible light with ozone on honeycomb-like porous g-C_3N_4 towards superior oxidation of water pollutants. Appl Catal B 183:417–425. https://doi.org/10.1016/j.apcatb.2015.11.010
Xie T, Xu L, Liu C, Wang Y (2013) Magnetic composite $ZnFe_2O_4$/$SrFe_{12}O_{19}$: preparation, characterization, and photocatalytic activity under visible light. Appl Surf Sci 273:684–691. https://doi.org/10.1016/j.apsusc.2013.02.113
Xie L, Ni J, Tang B, He G, Chen H (2018) A self-assembled 2D/2D-type protonated carbon nitride-modified graphene oxide nanocomposite with improved photocatalytic activity. Appl Surf Sci 434:456–463. https://doi.org/10.1016/j.apsusc.2017.10.193
Xin Z, Li L, Zhang W, Sui T, Li Y, Zhang X (2018) Synthesis of ZnS@CdS–Te composites with *p–n* heterostructures for enhanced photocatalytic hydrogen production by microwave-assisted hydrothermal method. Mol Catal 447:1–12. https://doi.org/10.1016/j.mcat.2018.01.001
Xu J, Meng W, Zhang Y, Li L, Guo C (2011) Photocatalytic degradation of tetrabromobisphenol A by mesoporous BiOBr: efficacy, products and pathway. Appl Catal B 107:355–362. https://doi.org/10.1016/j.apcatb.2011.07.036
Xu J, Luo L, Xiao G, Zhang Z, Lin H, Wang X, Long J (2014) Layered $C_3N_3S_3$ polymer/graphene hybrids as metal-free catalysts for selective photocatalytic oxidation of benzylic alcohols under visible light. ACS Catal 4:3302–3306. https://doi.org/10.1021/cs5006597
Xu H, Wu Z, Ding M, Gao X (2017) Microwave-assisted synthesis of flower-like BN/BiOCl composites for photocatalytic Cr(VI) reduction upon visible-light irradiation. Mater Des 114:129–138. https://doi.org/10.1016/j.matdes.2016.10.057
Yahaya AH, Gondal MA, Hameed A (2004) Selective laser enhanced photocatalytic conversion of CO_2 into methanol. Chem Phys Lett 400:206–212. https://doi.org/10.1016/j.cplett.2004.10.109
Yan S, Li Z, Zou Z (2010) Photodegradation of rhodamine B and methyl orange over boron-doped g-C_3N_4 under visible light irradiation. Langmuir 26:3894–3901. https://doi.org/10.1021/la904023j
Yang H, Yan J, Lu Z, Cheng X, Tang Y (2009) Photocatalytic activity evaluation of tetragonal $CuFe_2O_4$ nanoparticles for the H_2 evolution under visible light irradiation. J Alloys Compd 476:715–719. https://doi.org/10.1016/j.jallcom.2008.09.104
Yang Z, Zhang J, Kintner-Meyer MC, Lu X, Choi D, Lemmon JP, Liu J (2011) Electrochemical energy storage for green grid. Chem Rev 111:3577–3613. https://doi.org/10.1021/cr100290v
Yang X, Qian F, Zou G, Li M, Lu J, Li Y, Bao M (2016) Facile fabrication of acidified g-C_3N_4/g-C_3N_4 hybrids with enhanced photocatalysis performance under visible light irradiation. Appl Catal B 193:22–35. https://doi.org/10.1016/j.apcatb.2016.03.060
Yang M, Yang Q, Zhong J, Li J, Huang S, Li X (2017) PVA-assisted hydrothermal preparation of BiOF with remarkably enhanced photocatalytic performance. Mater Lett 201:35–38. https://doi.org/10.1016/j.matlet.2017.04.125
Yang Q, Chen Z, Yang X, Zhou D, Qian X, Zhang J, Zhang D (2018) Facile synthesis of Si_3N_4 nanowires with enhanced photocatalytic application. Mater Lett 212:41–44. https://doi.org/10.1016/j.matlet.2017.10.045
Yao Y, Lu F, Zhu Y, Wei F, Liu X, Lian C, Wang S (2015) Magnetic core–shell $CuFe_2O_4$@C_3N_4 hybrids for visible light photocatalysis of Orange II. J Hazard Mater 297:224–233. https://doi.org/10.1016/j.jhazmat.2015.04.046
Yao Z, Qiao X, Liu D, Shi Y, Zhao Y (2016) Catalytic activities of transition metal phosphides for NO dissociation and reduction with CO. Chem Biochem Eng Q 29:505–510. https://doi.org/10.15255/CABEQ.2014.2133
Ye D, Li D, Zhang W, Sun M, Hu Y, Zhang Y, Fu X (2008) A new photocatalyst $CdWO_4$ prepared with a hydrothermal method. J Phys Chem C 112:17351–17356. https://doi.org/10.1021/jp8059213
Ye L, Deng K, Xu F, Tian L, Peng T, Zan L (2012) Increasing visible-light absorption for photocatalysis with black BiOCl. Phys Chem Chem Phys 14:82–85. https://doi.org/10.1039/C1CP22876E
Yin LW, Bando Y, Zhu YC, Li MS (2004) Controlled carbon nanotube sheathing on ultrafine InP nanowires. Appl Phys Lett 84:5314–5316. https://doi.org/10.1063/1.1766079
Yu Z, Meng J, Xiao J, Li Y, Li Y (2014) Cobalt sulfide quantum dots modified TiO_2 nanoparticles for efficient photocatalytic hydrogen evolution. Int J Hydrogen Energy 39:15387–15393. https://doi.org/10.1016/j.ijhydene.2014.07.165
Yu Y, Yu C, Xu T, Sun H (2017a) Optical and photocatalytic properties of indium phosphide nanoneedles and nanotubes. Mater Sci Semicond Process 68:270–274. https://doi.org/10.1016/j.mssp.2017.06.036
Yu Z, Li F, Yang Q, Shi H, Chen Q, Xu M (2017b) Nature-mimic method to fabricate polydopamine/graphitic carbon nitride for

enhancing photocatalytic degradation performance. ACS Sustain Chem Eng 5:7840–7850. https://doi.org/10.1021/acssuschemeng.7b01313

Yu J et al (2018) Synthesis of carbon-doped $KNbO_3$ photocatalyst with excellent performance for photocatalytic hydrogen production. Sol Energy Mater Sol Cells 179:45–56. https://doi.org/10.1016/j.solmat.2018.01.043

Yuan X et al (2016) Facile synthesis of 3D porous thermally exfoliated g-C_3N_4 nanosheet with enhanced photocatalytic degradation of organic dye. J Colloid Interface Sci 468:211–219. https://doi.org/10.1016/j.jcis.2016.01.048

Yuliati L, Yang J-H, Wang X, Maeda K, Takata T, Antonietti M, Domen K (2010) Highly active tantalum(V) nitride nanoparticles prepared from a mesoporous carbon nitride template for photocatalytic hydrogen evolution under visible light irradiation. J Mater Chem 20:4295–4298. https://doi.org/10.1039/C0JM00341G

Yungi L, Kota N, Tomoaki W, Tsuyoshi T, Michikazu H, Masahiro Y, Kazunari D (2006) Effect of 10 MPa ammonia treatment on the activity of visible light responsive Ta_3N_5 photocatalyst. Chem Lett 35:352–353. https://doi.org/10.1246/cl.2006.352

Zainal Z, Hussein MZ, Ghazali A (1996) Cathodic electrodeposition of SnS thin films from aqueous solution. Sol Energy Mater Sol Cells 40:347–357. https://doi.org/10.1016/0927-0248(95)00157-3

Zarghami Z, Ebadi M, Motevalli K, Aliabadi M (2016) Self-assembly of nanoparticles to prepare of dendritic AgCl–Ag_2S nanocomposites through a simple one-pot hydrothermal approach and its photocatalytic activity. J Mater Sci Mater Electron 27:1087–1091. https://doi.org/10.1007/s10854-015-3855-9

Zhang K, Guo L (2013) Metal sulphide semiconductors for photocatalytic hydrogen production. Catal Sci Technol 3:1672–1690. https://doi.org/10.1039/C3CY00018D

Zhang K-L, Liu C-M, Huang F-Q, Zheng C, Wang W-D (2006) Study of the electronic structure and photocatalytic activity of the BiOCl photocatalyst. Appl Catal B 68:125–129. https://doi.org/10.1016/j.apcatb.2006.08.002

Zhang H, Chen G, Li Y, Teng Y (2010) Electronic structure and photocatalytic properties of copper-doped $CaTiO_3$. Int J Hydrogen Energy 35:2713–2716. https://doi.org/10.1016/j.ijhydene.2009.04.050

Zhang G, Zhang J, Zhang M, Wang X (2012) Polycondensation of thiourea into carbon nitride semiconductors as visible light photocatalysts. J Mater Chem 22:8083–8091. https://doi.org/10.1039/C2JM00097K

Zhang D, Pu X, Gao Y, Su C, Li H, Li H, Hang W (2013) One-step combustion synthesis of $CoFe_2O_4$–graphene hybrid materials for photodegradation of methylene blue. Mater Lett 113:179–181. https://doi.org/10.1016/j.matlet.2013.09.088

Zhang D et al (2014a) Combustion synthesis of magnetic Ag/$NiFe_2O_4$ composites with enhanced visible-light photocatalytic properties. Sep Purif Technol 137:82–85. https://doi.org/10.1016/j.seppur.2014.09.025

Zhang L, Song Y, Feng J, Fang T, Zhong Y, Li Z, Zou Z (2014b) Photoelectrochemical water oxidation of $LaTaON_2$ under visible-light irradiation. Int J Hydrogen Energy 39:7697–7704. https://doi.org/10.1016/j.ijhydene.2014.02.177

Zhang S, Zhang S, Song L, Wei Q (2014c) A general approach to the synthesis of metal phosphide catalysts. Powder Technol 253:509–513. https://doi.org/10.1016/j.powtec.2013.12.002

Zhang J, Yao W, Huang C, Shi P, Xu Q (2017a) High efficiency and stable tungsten phosphide cocatalysts for photocatalytic hydrogen production. J Mater Chem A 5:12513–12519. https://doi.org/10.1039/C7TA02297B

Zhang W, Zhou L, Shi J, Deng H (2017b) Fabrication of novel visible-light-driven AgI/g-C_3N_4 composites with enhanced visible-light photocatalytic activity for diclofenac degradation. J Colloid Interface Sci 496:167–176. https://doi.org/10.1016/j.jcis.2017.02.022

Zhang Z, Xiao A, Yan K, Liu Y, Yan Z, Chen J (2017c) $CuInS_2$/ZnS/TGA nanocomposite photocatalysts: synthesis characterization and photocatalytic activity. Catal Lett 147:1631–1639. https://doi.org/10.1007/s10562-017-2067-8

Zhang F, Zhuang H-Q, Song J, Men Y-L, Pan Y-X, Yu S-H (2018a) Coupling cobalt sulfide nanosheets with cadmium sulfide nanoparticles for highly efficient visible-light-driven photocatalysis. Appl Catal B 226:103–110. https://doi.org/10.1016/j.apcatb.2017.12.046

Zhang L et al (2018b) Preparation of upconversion Yb^{3+} doped microspherical BiOI with promoted photocatalytic performance. Solid State Sci 75:45–52. https://doi.org/10.1016/j.solidstatesciences.2017.11.008

Zhang W, Dong XA, Jia B, Zhong J, Sun Y, Dong F (2018c) 2D BiOCl/$Bi_{12}O_{17}Cl_2$ nanojunction: enhanced visible light photocatalytic NO removal and in situ DRIFTS investigation. Appl Surf Sci 430:571–577. https://doi.org/10.1016/j.apsusc.2017.06.186

Zhang X, Guo Y, Tian J, Sun B, Liang Z, Xu X, Cui H (2018d) Controllable growth of MoS_2 nanosheets on novel Cu_2S snowflakes with high photocatalytic activity. Appl Catal B 232:355–364. https://doi.org/10.1016/j.apcatb.2018.03.074

Zhao Z, Sun Y, Dong F (2015) Graphitic carbon nitride based nanocomposites: a review. Nanoscale 7:15–37. https://doi.org/10.1039/C4NR03008G

Zhao R, Li X, Lin K, Gao X (2016a) Preparation and photocatalytic performance of the Mn/BiOCl albizia flower. Res Chem Intermed 42:7031–7043. https://doi.org/10.1007/s11164-016-2514-y

Zhao Y, Jia X, Waterhouse GI, Wu LZ, Tung CH, O'Hare D, Zhang T (2016b) Layered double hydroxide nanostructured photocatalysts for renewable energy production. Adv Energy Mater. https://doi.org/10.1002/aenm.201501974

Zhao S, Guo T, Li X, Xu T, Yang B, Zhao X (2018a) Carbon nanotubes covalent combined with graphitic carbon nitride for photocatalytic hydrogen peroxide production under visible light. Appl Catal B 224:725–732. https://doi.org/10.1016/j.apcatb.2017.11.005

Zhao Y, Wang Y, Liu E, Fan J, Hu X (2018b) Bi_2WO_6 nanoflowers: an efficient visible light photocatalytic activity for ceftriaxone sodium degradation. Appl Surf Sci 436:854–864. https://doi.org/10.1016/j.apsusc.2017.12.064

Zhu M, Zhai C, Fujitsuka M, Majima T (2018) Noble metal-free near-infrared-driven photocatalyst for hydrogen production based on 2D hybrid of black Phosphorus/WS_2. Appl Catal B 221:645–651. https://doi.org/10.1016/j.apcatb.2017.09.063